CHAPTER

Special Topics 10

This chapter briefly introduces some special topics in fracture mechanics, including fracture of anisotropic solids, fracture of nonhomegenous matertials, and dynamic fracture mechanics. In recent years, fiber-reinforced composite materials have found wide applications in aerospace, automotive, civil infrastructures, sports equipment, and other industries. Damage tolerance and defect assessments for the structural integrity of composite structures require thorough understanding of fracture behavior of composites. Fracture mechanics of nonhomogeneous materials has applications in macroscopically heterogeneous materials such as functionally graded materials (FGMs), which have been developed to meet the increasing multifunctional structural performance requirements in engineering applications. Many engineering structures are subjected to dynamic loads such as explosive loads, wind loads, impact by foreign objects, and so on. Prediction of crack initiation and propagation in a dynamically loaded structure must be based on dynamic fracture mechanics, which generally considers both inertia effects on the stresses and displacements, and loading rate effects on the constitutive responses of materials.

10.1 FRACTURE MECHANICS OF ANISOTROPIC SOLIDS

Composite materials, or simply composites, include fiber- and particulate-reinforced materials. Composites are heterogeneous materials at the microscopic scale. In continuum mechanics, properties of a composite are homogenized at the macroscopic level and the material is treated as a macroscopically, or statistically homogeneous material. The most successful composites for aerospace and other engineering applications have been fiber-reinforced polymer matrix materials. Fiber composites are usually modeled as anisotropic materials with three mutually orthogonal planes of symmerty. This section focuses on the fracture of fiber-reinforced materials. The composites are treated as anisotropic materials at the macroscopic level.

Fracture Mechanics. DOI: 10.1016/B978-0-12-385001-0.00010-9

10.1.1 Basic Plane Elasticity Equations of Anisotropic Solids

The constitutive relations for a general anisotropic material are given by the matrix form

$$\{e\} = [a]\{\sigma\} \tag{10.1}$$

where $\{\sigma\}$ and $\{e\}$ are the arrays of stresses and strains defined by

$$\{\sigma\} = [\sigma_{xx}\ \sigma_{yy}\ \sigma_{zz}\ \sigma_{yz}\ \sigma_{xz}\ \sigma_{xy}]^T \tag{10.2}$$

$$\{e\} = [e_{xx}\ e_{yy}\ e_{zz}\ 2e_{yz}\ 2e_{xz}\ 2e_{xy}]^T \tag{10.3}$$

and $[a] = \{a_{ij}\}$ $(i,j = 1,2,...,6)$ is the elastic compliance matrix. If the $x-y$ plane is a plane of symmetry, then for the state of plane stress, $\sigma_z = \sigma_{yz} = \sigma_{xz} = 0$, and these constitutive equations reduce to

$$\begin{aligned} e_{xx} &= a_{11}\sigma_{xx} + a_{12}\sigma_{yy} + a_{16}\sigma_{xy} \\ e_{yy} &= a_{12}\sigma_{xx} + a_{22}\sigma_{yy} + a_{26}\sigma_{xy} \\ 2e_{xy} &= a_{16}\sigma_{xx} + a_{26}\sigma_{yy} + a_{66}\sigma_{xy} \end{aligned} \tag{10.4}$$

with the out-of-plane normal strain given by $e_{zz} = a_{31}\sigma_{xx} + a_{32}\sigma_{yy} + a_{36}\sigma_{xy}$. The corresponding constitutive equations for the state of plane strain parallel to the $x-y$ plane are

$$\begin{aligned} e_{xx} &= b_{11}\sigma_{xx} + b_{12}\sigma_{yy} + b_{16}\sigma_{xy} \\ e_{yy} &= b_{21}\sigma_{xx} + b_{22}\sigma_{yy} + b_{26}\sigma_{xy} \\ 2e_{xy} &= b_{61}\sigma_{xx} + b_{62}\sigma_{yy} + b_{66}\sigma_{xy} \end{aligned} \tag{10.5}$$

in which

$$b_{11} = \left(a_{11}a_{33} - a_{13}^2\right)/a_{33}, \quad b_{12} = b_{21} = \left(a_{12}a_{33} - a_{13}a_{23}\right)/a_{33}$$

$$b_{22} = \left(a_{22}a_{33} - a_{23}^2\right)/a_{33}, \quad b_{16} = b_{61} = \left(\left(a_{16}a_{33} - a_{13}a_{36}\right)/a_{33}\right.$$

$$b_{66} = \left(a_{66}a_{33} - a_{36}^2\right)/a_{33}, \quad b_{26} = b_{62} = \left(a_{26}a_{33} - a_{23}a_{36}\right)/a_{33}$$

Using the Airy stress function ϕ,

$$\sigma_{xx} = \frac{\partial^2\phi}{\partial y^2}, \quad \sigma_{xy} = -\frac{\partial^2\phi}{\partial x \partial y}, \quad \sigma_{yy} = \frac{\partial^2\phi}{\partial x^2}$$

and the plane stress constitutive relations Eq. (10.4) can be written as

$$e_{xx} = a_{11}\frac{\partial^2\phi}{\partial y^2} + a_{12}\frac{\partial^2\phi}{\partial x^2} - a_{16}\frac{\partial^2\phi}{\partial x\partial y}$$

$$e_{yy} = a_{12}\frac{\partial^2\phi}{\partial y^2} + a_{22}\frac{\partial^2\phi}{\partial x^2} - a_{26}\frac{\partial^2\phi}{\partial x\partial y}$$

$$2e_{xy} = a_{16}\frac{\partial^2\phi}{\partial y^2} + a_{26}\frac{\partial^2\phi}{\partial x^2} - a_{66}\frac{\partial^2\phi}{\partial x\partial y}$$

Substituting these equations in the following compatibility equation of strains:

$$\frac{\partial^2 e_{xx}}{\partial y^2} + \frac{\partial^2 e_{yy}}{\partial x^2} = 2\frac{\partial^2 e_{xy}}{\partial x\partial y}$$

we obtain the governing equation of the Airy stress function as follows:

$$a_{22}\frac{\partial^4\phi}{\partial x^4} - 2a_{26}\frac{\partial^4\phi}{\partial x^3\partial y} + (2a_{12}+a_{66})\frac{\partial^4\phi}{\partial x^2\partial y^2} - 2a_{16}\frac{\partial^4\phi}{\partial x\partial y^3} + a_{11}\frac{\partial^4\phi}{\partial y^4} = 0 \quad (10.6)$$

This equation may be written in the following form (Lekhnitskii [10-1]):

$$\left(\frac{\partial}{\partial y} - s_1\frac{\partial}{\partial x}\right)\left(\frac{\partial}{\partial y} - s_2\frac{\partial}{\partial x}\right)\left(\frac{\partial}{\partial y} - s_3\frac{\partial}{\partial x}\right)\left(\frac{\partial}{\partial y} - s_4\frac{\partial}{\partial x}\right)\phi = 0 \quad (10.7)$$

where the constants s_i $(i = 1,2,3,4)$ are the roots of the following characteristic equation:

$$a_{11}s^4 - 2a_{16}s^3 + (2a_{12}+a_{66})s^2 - 2a_{26}s + a_{22} = 0 \quad (10.8)$$

These roots are either complex or pure imaginary according to Lekhnitskii [10-1] and can be written as

$$s_1 = \alpha_1 + i\beta_1$$
$$s_2 = \alpha_2 + i\beta_2$$
$$s_3 = \bar{s}_1 = \alpha_1 - i\beta_1$$
$$s_4 = \bar{s}_2 = \alpha_2 - i\beta_2$$

For anisotropic materials with distinct roots, the general solution of Eq. (10.7) can be expressed in terms of two complex functions $F_1(z_1)$ and $F_2(z_2)$ as follows:

$$\phi = 2\,\mathrm{Re}[F_1(z_1) + F_2(z_2)] \quad (10.9)$$

where z_1 and z_2 are defined by

$$z_1 = x + s_1 y, \qquad z_2 = x + s_2 y$$

Hence, the stresses and displacements have the following expressions [10-1]:

$$\begin{aligned} \sigma_{xx} &= 2\mathrm{Re}\left[s_1^2\psi'(z_1) + s_2^2\chi'(z_2)\right] \\ \sigma_{yy} &= 2\mathrm{Re}\left[\psi'(z_1) + \chi'(z_2)\right] \\ \sigma_{xy} &= -2\mathrm{Re}\left[s_1\psi'(z_1) + s_2\chi'(z_2)\right] \end{aligned} \tag{10.10}$$

$$\begin{aligned} u_x &= 2\mathrm{Re}[p_1\psi(z_1) + p_2\chi(z_2)] \\ u_y &= 2\mathrm{Re}[q_1\psi(z_1) + q_2\chi(z_2)] \end{aligned} \tag{10.11}$$

where

$$\psi(z_1) = F_1'(z_1), \qquad \chi(z_2) = F_2'(z_2)$$

$$p_1 = a_{11}s_1^2 + a_{12} - a_{16}s_1, \qquad p_2 = a_{11}s_2^2 + a_{12} - a_{16}s_2$$
$$q_1 = a_{12}s_1 + a_{22}/s_1 - a_{26}, \qquad q_2 = a_{12}s_2 + a_{22}/s_2 - a_{26}$$

10.1.2 A Mode I Crack in an Infinite Anisotropic Plate under Uniform Crack Surface Pressure

Sih and Liebowitz [10-2] studied a Mode I crack of length $2a$ in an infinite anisotropic plate (see Figure 10.1) subjected to a uniform pressure σ_0 on the crack surfaces based on Lekhnitskii's complex potential formulations described earlier. The material properties need to be symmetrical about the crack line. In other words, the $x - y$ and $x - z$

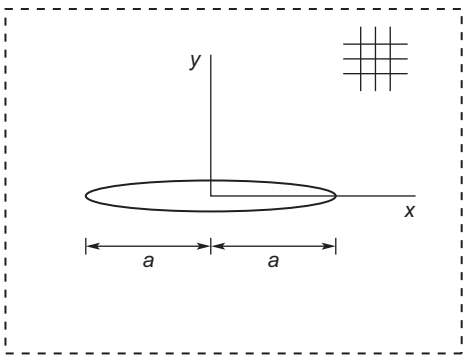

FIGURE 10.1

A crack in an infinite anisotropic plate.

planes are two mutually orthogonal planes of symmetry. Sih and Liebowitz [10-2] obtained the following complex potentials for the crack problem:

$$\psi'(z_1) = -\frac{s_2}{s_1 - s_2}\frac{\sigma_0}{2\sqrt{z_1^2 - a^2}}\left[z_1 - \sqrt{z_1^2 - a^2}\right]$$
$$\chi'(z_2) = \frac{s_1}{s_1 - s_2}\frac{\sigma_0}{2\sqrt{z_2^2 - a^2}}\left[z_2 - \sqrt{z_2^2 - a^2}\right] \tag{10.12}$$

The stresses and displacements near the crack tip ($x = a$, $y = 0$) can be obtained by substituting the preceding potentials into Eqs. (10.10) and (10.11), respectively, as follows

$$\sigma_{xx} = \frac{K_I}{\sqrt{2\pi r}}\mathrm{Re}\left[\frac{s_1 s_2}{s_1 - s_2}\left(\frac{s_2}{\sqrt{\cos\theta + s_2\sin\theta}} - \frac{s_1}{\sqrt{\cos\theta + s_1\sin\theta}}\right)\right]$$
$$\sigma_{yy} = \frac{K_I}{\sqrt{2\pi r}}\mathrm{Re}\left[\frac{1}{s_1 - s_2}\left(\frac{s_1}{\sqrt{\cos\theta + s_2\sin\theta}} - \frac{s_2}{\sqrt{\cos\theta + s_1\sin\theta}}\right)\right] \tag{10.13}$$
$$\sigma_{xy} = \frac{K_I}{\sqrt{2\pi r}}\mathrm{Re}\left[\frac{s_1 s_2}{s_1 - s_2}\left(\frac{1}{\sqrt{\cos\theta + s_1\sin\theta}} - \frac{1}{\sqrt{\cos\theta + s_2\sin\theta}}\right)\right]$$

$$u_x = K_I\sqrt{\frac{2r}{\pi}}\mathrm{Re}\left[\frac{1}{s_1 - s_2}\left(s_1 p_2\sqrt{\cos\theta + s_2\sin\theta} - s_2 p_1\sqrt{\cos\theta + s_1\sin\theta}\right)\right]$$
$$u_y = K_I\sqrt{\frac{2r}{\pi}}\mathrm{Re}\left[\frac{1}{s_1 - s_2}\left(s_1 q_2\sqrt{\cos\theta + s_2\sin\theta} - s_2 q_1\sqrt{\cos\theta + s_1\sin\theta}\right)\right] \tag{10.14}$$

where $K_I = \sigma_0\sqrt{\pi a}$ is the Mode I stress intensity factor (SIF), and (r,θ) are the polar coordinates centered at the crack tip. Clearly, the stresses still have the inverse square root singularity and the SIF is the same as that for an isotropic material in this special case. The angular distributions of the stresses, however, depend on the elastic constants via s_1 and s_2.

10.1.3 A Mode II Crack in an Infinite Anisotropic Plate under Uniform Crack Surface Shear

Sih and Liebowitz [10-2] also considered a Mode II crack of length $2a$ in an infinite anisotropic plate subjected to uniform crack surface shearing τ_0. The material properties are still symmetrical about the crack line. The complex potentials for the crack

problem are given by

$$\psi'(z_1) = -\frac{1}{s_1 - s_2}\frac{\tau_0}{2\sqrt{z_1^2 - a^2}}\left[z_1 - \sqrt{z_1^2 - a^2}\right]$$
$$\chi'(z_2) = \frac{1}{s_1 - s_2}\frac{\tau_0}{2\sqrt{z_2^2 - a^2}}\left[z_2 - \sqrt{z_2^2 - a^2}\right] \tag{10.15}$$

Substituting these potentials into Eqs. (10.10) and (10.11), one can obtain the stresses and displacements near the crack tip ($x = a$, $y = 0$) as follows [10-2]:

$$\sigma_{xx} = \frac{K_{II}}{\sqrt{2\pi r}}\mathrm{Re}\left[\frac{1}{s_1 - s_2}\left(\frac{s_2^2}{\sqrt{\cos\theta + s_2\sin\theta}} - \frac{s_1^2}{\sqrt{\cos\theta + s_1\sin\theta}}\right)\right]$$
$$\sigma_{yy} = \frac{K_{II}}{\sqrt{2\pi r}}\mathrm{Re}\left[\frac{1}{s_1 - s_2}\left(\frac{1}{\sqrt{\cos\theta + s_2\sin\theta}} - \frac{1}{\sqrt{\cos\theta + s_1\sin\theta}}\right)\right] \tag{10.16}$$
$$\sigma_{xy} = \frac{K_{II}}{\sqrt{2\pi r}}\mathrm{Re}\left[\frac{1}{s_1 - s_2}\left(\frac{s_1}{\sqrt{\cos\theta + s_1\sin\theta}} - \frac{s_2}{\sqrt{\cos\theta + s_2\sin\theta}}\right)\right]$$

$$u_x = K_{II}\sqrt{\frac{2r}{\pi}}\mathrm{Re}\left[\frac{1}{s_1 - s_2}\left(p_2\sqrt{\cos\theta + s_2\sin\theta} - p_1\sqrt{\cos\theta + s_1\sin\theta}\right)\right]$$
$$u_y = K_{II}\sqrt{\frac{2r}{\pi}}\mathrm{Re}\left[\frac{1}{s_1 - s_2}\left(q_2\sqrt{\cos\theta + s_2\sin\theta} - q_1\sqrt{\cos\theta + s_1\sin\theta}\right)\right] \tag{10.17}$$

where $K_{II} = \tau_0\sqrt{\pi a}$ is the Mode II SIF.

10.1.4 Energy Release Rate

Using the crack closure integral technique, the Mode I energy release rate may be determined from

$$G_I = \lim_{\Delta a \to 0}\frac{1}{\Delta a}\int_0^{\Delta a}\sigma_{yy}(x,0)u_y(\Delta a - x,\pi)dx \tag{10.18}$$

where $\sigma_{yy}(x,0)$ is the stress when the crack tip is at $x = 0$, and $u_y(\Delta a - x,\pi)$ is the displacement of the upper crack face when the crack tip is at $x = \Delta a$. Substituting the crack tip stress Eq. (10.13) and displacement Eq. (10.14) in the preceding equation, the energy release rates can be evaluated as follows:

$$G_I = -\frac{K_I^2}{2}a_{22}\,\mathrm{Im}\left[\frac{s_1 + s_2}{s_1 s_2}\right] \tag{10.19}$$

Similarly, the Mode II energy release rate can be derived as

$$G_{II} = \lim_{\Delta a \to 0} \frac{1}{\Delta a} \int_0^{\Delta a} \sigma_{xy}(x,0) u_x(\Delta a - x, \pi) dx = \frac{K_{II}^2}{2} a_{11} \operatorname{Im}[s_1 + s_2] \tag{10.20}$$

For the special case of orthotropic materials with the $x-z$ and $y-z$ planes as symmetry planes, $a_{16} = a_{26} = 0$ and the roots s_1 and s_2 become

$$s_1^2 = -\frac{2a_{12} + a_{66}}{2a_{11}} + \frac{1}{2a_{11}} \sqrt{(2a_{12} + a_{66})^2 - 4a_{11}a_{22}}$$
$$s_2^2 = -\frac{2a_{12} + a_{66}}{2a_{11}} - \frac{1}{2a_{11}} \sqrt{(2a_{12} + a_{66})^2 - 4a_{11}a_{22}}$$

The energy release rates now reduce to

$$\begin{aligned} G_I &= K_I^2 \sqrt{\frac{a_{11}a_{22}}{2}} \sqrt{\left[\frac{2a_{12} + a_{66}}{2a_{11}} + \sqrt{\frac{a_{22}}{a_{11}}} \right]} \\ G_{II} &= K_{II}^2 \frac{a_{11}}{\sqrt{2}} \sqrt{\left[\frac{2a_{12} + a_{66}}{2a_{11}} + \sqrt{\frac{a_{22}}{a_{11}}} \right]} \end{aligned} \tag{10.21}$$

The elastic compliances are related to the engineering moduli of the composite as

$$a_{11} = \frac{1}{E_x}, \qquad a_{22} = \frac{1}{E_y}, \qquad a_{12} = -\frac{\nu_{yx}}{E_y}, \qquad a_{66} = \frac{1}{\mu_{xy}} \tag{10.22}$$

where E_x and E_y are the elastic moduli in the x- and y-directions, respectively, and μ_{xy} and ν_{yx} are the shear modulus and Poisson's ratio in the $x-y$ plane, respectively.

10.2 FRACTURE MECHANICS OF NONHOMOGENEOUS MATERIALS

Conventional composite materials are macroscopically, or statistically homogeneous materials. In a macroscopically nonhomogeneous material, or simply nonhomogeneous material, material properties vary with spatial position. Natural materials such as bones and bamboos are nonhomogeneous materials. Engineering materials in a field of elevated nonuniform temperature are also nonhomogeneous as material properties are temperature-dependent.

Recent progress in fracture mechanics of nonhomogeneous materials is largely owed to the development of FGMs. Broadly speaking, FGMs are materials with graded microstructures and macroproperties. For high-performance structural applications, FGMs are often multiphased materials with the volume fractions of their

constituents varied gradually in predetermined profiles. This chapter introduces some basic concepts of fracture mechanics of nonhomogeous elastic materials, including FGMs.

10.2.1 Basic Plane Elasticity Equations of Nonhomogenous Materials

The basic equations of nonhomogeneous materials have the same forms as those for homogeneous solids except that the material properties are functions of spatial position. In plane elasticity of nonhomogeneous materials, Hooke's law with spatial position-dependent elasticity coefficients can be written as

$$\begin{aligned}\sigma_{xx} &= \lambda^*(x,y)\left(e_{xx}+e_{yy}\right)+2\mu(x,y)e_{xx}\\ \sigma_{yy} &= \lambda^*(x,y)\left(e_{xx}+e_{yy}\right)+2\mu(x,y)e_{yy}\\ \sigma_{xy} &= 2\mu(x,y)e_{xy}\end{aligned} \tag{10.23}$$

where $\lambda(x,y)$ and $\mu(x,y)$ are the spatial position-dependent Lame's constants, which are related to Young's modulus $E(x,y)$ and Poisson's ratio $\nu(x,y)$ by

$$\lambda(x,y)=\frac{E(x,y)\nu(x,y)}{[1+\nu(x,y)][1-2\nu(x,y)]},\qquad \mu(x,y)=\frac{E(x,y)}{2[1+\nu(x,y)]}$$

and $\lambda^*(x,y)$ is given by

$$\lambda^*=\begin{cases}\lambda & \text{for plane strain}\\ \dfrac{2\lambda\mu}{\lambda+2\mu} & \text{for plane stress}\end{cases}$$

The inverse form of Eq. (10.23) can be expressed as follows:

$$\begin{aligned}e_{xx} &= \frac{1}{2\mu(x,y)}\left[\sigma_{xx}-\frac{\lambda^*(x,y)}{2\left(\lambda^*(x,y)+\mu(x,y)\right)}\left(\sigma_{xx}+\sigma_{yy}\right)\right]\\ e_{yy} &= \frac{1}{2\mu(x,y)}\left[\sigma_{yy}-\frac{\lambda^*(x,y)}{2\left(\lambda^*(x,y)+\mu(x,y)\right)}\left(\sigma_{xx}+\sigma_{yy}\right)\right]\\ e_{xy} &= \frac{1}{2\mu(x,y)}\sigma_{xy}\end{aligned} \tag{10.24}$$

In the continuum analysis of graded composites, the elastic properties can be calculated from a micromechanics model (e.g., the Mori-Tanaka model derived by Weng [10-3]), or can be assumed to follow some elementary functions that are consistent with micromechanics analyses. An exponentially varying Young's modulus and a constant Poisson's ratio are frequently used, which leads to constant coefficient, partial differential equations for the displacement fields.

In addition to the constitutive law, the equilibrium equations,

$$\begin{aligned}\frac{\partial \sigma_{xx}}{\partial x}+\frac{\partial \sigma_{xy}}{\partial y}&=0\\ \frac{\partial \sigma_{xy}}{\partial x}+\frac{\partial \sigma_{yy}}{\partial y}&=0\end{aligned} \tag{10.25}$$

and the strain-displacement relations,

$$e_{xx}=\frac{\partial u_x}{\partial x},\quad e_{yy}=\frac{\partial u_y}{\partial y},\quad e_{xy}=\frac{1}{2}\left(\frac{\partial u_x}{\partial y}+\frac{\partial u_y}{\partial x}\right) \tag{10.26}$$

should also be satisfied.

By eliminating stresses and strains in Eqs. (10.23), (10.25), and (10.26), we can obtain the following governing equations for the displacements u_x and u_y:

$$\begin{aligned}&(\lambda^*+\mu)\frac{\partial}{\partial x}\left(\frac{\partial u_x}{\partial x}+\frac{\partial u_y}{\partial y}\right)+\mu\nabla^2 u_x\\ &\quad+\frac{\partial \lambda^*}{\partial x}\left(\frac{\partial u_x}{\partial x}+\frac{\partial u_y}{\partial y}\right)+2\frac{\partial \mu}{\partial x}\frac{\partial u_x}{\partial x}+\frac{\partial \mu}{\partial y}\left(\frac{\partial u_x}{\partial y}+\frac{\partial u_y}{\partial x}\right)=0,\\ &(\lambda^*+\mu)\frac{\partial}{\partial y}\left(\frac{\partial u_x}{\partial x}+\frac{\partial u_y}{\partial y}\right)+\mu\nabla^2 u_y\\ &\quad+\frac{\partial \lambda^*}{\partial y}\left(\frac{\partial u_x}{\partial x}+\frac{\partial u_y}{\partial y}\right)+2\frac{\partial \mu}{\partial y}\frac{\partial u_y}{\partial y}+\frac{\partial \mu}{\partial x}\left(\frac{\partial u_x}{\partial y}+\frac{\partial u_y}{\partial x}\right)=0\end{aligned} \tag{10.27}$$

where ∇^2 is the Laplace operator. For a nonhomogeneous material with exponentially graded modulus and constant Poisson's ratio, that is,

$$\mu=\mu_0\exp(\beta x+\gamma y),\qquad \nu=\nu_0 \tag{10.28}$$

where μ_0,ν_0,β, and γ are material constants, the governing equations (10.27) for the displacements reduce to

$$\begin{aligned}&(\kappa+1)\frac{\partial^2 u_x}{\partial x^2}+(\kappa-1)\frac{\partial^2 u_x}{\partial y^2}+2\frac{\partial u_y}{\partial x\partial y}+\beta(\kappa+1)\frac{\partial u_x}{\partial x}\\ &\quad+\gamma(\kappa-1)\frac{\partial u_x}{\partial y}+\gamma(\kappa-1)\frac{\partial u_y}{\partial x}+\beta(3-\kappa)\frac{\partial u_y}{\partial y}=0,\\ &(\kappa-1)\frac{\partial^2 u_y}{\partial x^2}+(\kappa+1)\frac{\partial^2 u_y}{\partial y^2}+2\frac{\partial u_x}{\partial x\partial y}+\gamma(3-\kappa)\frac{\partial u_x}{\partial x}\\ &\quad+\beta(\kappa-1)\frac{\partial u_x}{\partial y}+\beta(\kappa-1)\frac{\partial u_y}{\partial x}+\gamma(\kappa+1)\frac{\partial u_y}{\partial y}=0\end{aligned} \tag{10.29}$$

where $\kappa = 3 - 4\nu_0$ for plane strain, and $\kappa = (3 - \nu_0)/(1 + \nu_0)$ for plane stress. The equations in Eq. (10.29) are constant coefficient, partial differential equations that could be treated analytically or semi-analytically.

Equation (10.27) is used in the displacement method for plane elasticity of nonhomogeneous materials. Equivalently, a stress function method can be adopted. In this case, stresses are expressed in terms of the Airy stress function ϕ as follows:

$$\sigma_{xx} = \frac{\partial^2 \phi}{\partial y^2}, \qquad \sigma_{yy} = \frac{\partial^2 \phi}{\partial x^2}, \qquad \sigma_{xy} = -\frac{\partial^2 \phi}{\partial x \partial y} \tag{10.30}$$

The equlibrium equations (10.25) are satisfied with these stresses. Use of Hooke's law Eq. (10.24) and the strain-displacement relations Eq. (10.26) yields the governing equation of the Airy stress function for general nonhomogeneous materials under plane stress conditions:

$$\frac{1}{E}\nabla^2\nabla^2\phi + 2\left[\frac{\partial}{\partial x}\left(\frac{1}{E}\right)\frac{\partial \nabla^2 \phi}{\partial x} + \frac{\partial}{\partial y}\left(\frac{1}{E}\right)\frac{\partial \nabla^2 \phi}{\partial y}\right] + \nabla^2\left(\frac{1}{E}\right)\nabla^2\phi$$
$$- \frac{\partial^2}{\partial y^2}\left(\frac{1+\nu}{E}\right)\frac{\partial^2 \phi}{\partial x^2} - \frac{\partial^2}{\partial x^2}\left(\frac{1+\nu}{E}\right)\frac{\partial^2 \phi}{\partial y^2} + 2\frac{\partial^2}{\partial x \partial y}\left(\frac{1+\nu}{E}\right)\frac{\partial^2 \phi}{\partial x \partial y} = 0 \tag{10.31}$$

For plane strain, E and ν in this equation should be replaced by $E/(1-\nu^2)$ and $\nu/(1-\nu)$, respectively. Again, consider the nonhomogeneous material with a constant Poisson's ratio and an exponentially varying modulus Eq. (10.28). Now the basic equation of the Airy stress function Eq. (10.31) reduces to

$$\nabla^2\nabla^2\phi - 2\left(\beta\frac{\partial}{\partial x} + \gamma\frac{\partial}{\partial y}\right)\nabla^2\phi + \left(\beta^2 - \nu_0\gamma^2\right)\frac{\partial^2 \phi}{\partial x^2}$$
$$+ 2(1+\nu_0)\beta\gamma\frac{\partial^2 \phi}{\partial x \partial y} + \left(\gamma^2 - \nu_0\beta^2\right)\frac{\partial^2 \phi}{\partial y^2} = 0 \tag{10.32}$$

10.2.2 Crack Tip Stress and Displacement Fields

Consider a cracked nonhomogeneous material with continuous and piecewise differentiable Young's modulus E and Poisson's ratio ν. Here we assume there are only two differentiable pieces as shown in Figure 10.2, but the conclusion for the crack tip fields hold true for general cases. The boundary between the two differentiable pieces is referred to as the "weak property discontinuity line" (line L as shown in Figure 10.2). E and ν are continuously differentiable in each piece, continuous across the boundary L, and the derivatives of E and ν with respect to the spatial coordinates may undergo jumps across L. Assume that the crack terminates at the boundary L at an angle θ_L. The crack becomes an interface crack when θ_L equals 0 or π.

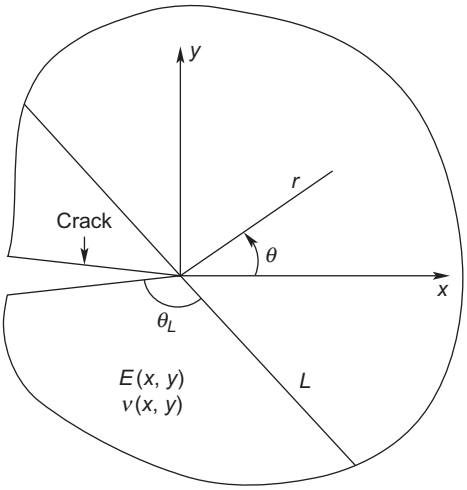

FIGURE 10.2

A crack in a nonhomogeneous medium.

To obtain the crack tip stress and deformation fields, assume the following asymptotic expansion of the Airy stress function in each differentiable piece near the crack tip (Jin and Noda [10-4]):

$$\begin{aligned}
&\phi = r^{s_1}\tilde{F}_1(\theta), \quad r \to 0, \quad -\pi < \theta < -(\pi - \theta_L),\\
&\phi = r^{s_2}\tilde{F}_2(\theta), \quad r \to 0, \quad -(\pi - \theta_L) < \theta < \theta_L,\\
&\phi = r^{s_3}\tilde{F}_3(\theta), \quad r \to 0, \quad \theta_L < \theta < \pi
\end{aligned} \tag{10.33}$$

where (r,θ) are the polar coordinates centered at the crack tip with $\theta = \pm\pi$ describing the crack faces, s_i $(i = 1,2,3)$ the eigenvalues to be determined, and $\tilde{F}_i$ $(i = 1,2,3)$ the unknown functions of θ. As the material is assumed to be piecewise differentiable, the elastic properties can be expanded into a Taylor series at the crack tip in each differentiable piece, that is,

$$\begin{aligned}
&E = E_{tip} + a_{11}x + b_{11}y + c_{11}x^2 + d_{11}xy + e_{11}y^2 + ..., \quad -\pi < \theta < -(\pi - \theta_L),\\
&E = E_{tip} + a_{12}x + b_{12}y + c_{12}x^2 + d_{12}xy + e_{12}y^2 + ..., \quad -(\pi - \theta_L) < \theta < \theta_L,\\
&E = E_{tip} + a_{13}x + b_{13}y + c_{13}x^2 + d_{13}xy + e_{13}y^2 + ..., \quad \theta_L < \theta < \pi
\end{aligned} \tag{10.34}$$

where $(x,y) = r(\cos\theta, \sin\theta)$ are the rectangular coordinates at the crack tip, E_{tip} is the Young's modulus at the crack tip, and a_{ij}, b_{ij}, c_{ij}, d_{ij}, and e_{ij} are constants related to the derivatives of the modulus at the crack tip in the differential pieces.

Similarly, the Poisson's ratio can also be expanded into a Taylor series in each differentiable piece. By substituting Eqs. (10.33) and (10.34) into the governing equation (10.31), we can find that the first term dominates the other terms, and hence the dominant term for the Airy stress function still satisfies the biharmonic equation in every differentiable piece, that is,

$$\nabla^2\nabla^2\phi = 0 \tag{10.35}$$

The singular solution to homogeneous materials (Williams [10-5]) satisfies the same equation. Thus, it is also the dominant solution to the nonhomogeneous material in every differentiable piece and satisfies the displacement and traction continuity conditions across the weak property discontinuity line as long as the material properties are continuous. Hence, we can come to the conclusion that the crack tip stress and displacement fields in nonhomogeneous materials have the same forms as those in homogeneous materials provided the material properties are continuous and piecewise differentiable. The elastic properties at the crack tip, however, should be used in the displacement field.

Eischen [10-6] considered a nonhomogeneous material with continuously differentiable properties and reached the same conclusion. Thus, the asymptotic crack tip stress and displacement fields in nonhomogeneous elastic materials can be written as ($r \to 0$)

$$\begin{aligned}
\sigma_{xx} &= \frac{K_I}{\sqrt{2\pi r}}\cos\frac{1}{2}\theta\left(1-\sin\frac{1}{2}\theta\sin\frac{3}{2}\theta\right)\\
&\quad -\frac{K_{II}}{\sqrt{2\pi r}}\sin\frac{1}{2}\theta\left(2+\cos\frac{\theta}{2}\cos\frac{3\theta}{2}\right)\\
\sigma_{yy} &= \frac{K_I}{\sqrt{2\pi r}}\cos\frac{1}{2}\theta\left(1+\sin\frac{1}{2}\theta\sin\frac{3}{2}\theta\right)\\
&\quad +\frac{K_{II}}{\sqrt{2\pi r}}\sin\frac{\theta}{2}\cos\frac{\theta}{2}\cos\frac{3}{2}\theta\\
\sigma_{xy} &= \frac{K_I}{\sqrt{2\pi r}}\sin\frac{1}{2}\theta\cos\frac{1}{2}\theta\cos\frac{3}{2}\theta\\
&\quad +\frac{K_{II}}{\sqrt{2\pi r}}\cos\frac{1}{2}\theta\left(1-\sin\frac{1}{2}\theta\sin\frac{3}{2}\theta\right)
\end{aligned} \tag{10.36}$$

and

$$\begin{aligned}
u_x &= \frac{K_I}{8\mu_{tip}\pi}\sqrt{2\pi r}\left[(2\kappa_{tip}-1)\cos\frac{\theta}{2}-\cos\frac{3\theta}{2}\right]\\
&\quad +\frac{K_{II}}{8\mu_{tip}\pi}\sqrt{2\pi r}\left[(2\kappa_{tip}+3)\sin\frac{\theta}{2}+\sin\frac{3\theta}{2}\right]
\end{aligned}$$

$$u_y = \frac{K_I}{8\mu_{tip}\pi}\sqrt{2\pi r}\left[(2\kappa_{tip}+1)\sin\frac{\theta}{2} - \sin\frac{3\theta}{2}\right] - \frac{K_{II}}{8\mu_{tip}\pi}\sqrt{2\pi r}\left[(2\kappa_{tip}-3)\cos\frac{\theta}{2} + \cos\frac{3\theta}{2}\right] \tag{10.37}$$

where K_I and K_{II} are Mode I and Mode II SIFs, respectively, and μ_{tip} and ν_{tip} are the shear modulus and Poisson's ratio at the crack tip, and κ_{tip} is given by

$$\kappa_{tip} = \begin{cases} 3-4\nu_{tip} & \text{for plane strain} \\ \dfrac{3-\nu_{tip}}{1+\nu_{tip}} & \text{for plane stress} \end{cases}$$

The previous result about the identity of the crack tip fields between homogeneous and nonhomogeneous materials is obtained under two-dimensional quasistatic, isotropic conditions. The conclusion holds true for general three-dimensional, anisotropic, and dynamic crack problems of nonhomogeneous materials. Equations (10.36) and (10.37) indicate that material nonhomogeneities influence the crack tip stress and displacement solutions only through SIFs. Because the crack tip stress and displacement fields have the same forms as those for homogeneous materials, the relation between the energy release rate G and SIFs for nonhomogeneous materials also have the form

$$G = \frac{1}{E^*_{tip}}\left(K_I^2 + K_{II}^2\right)$$

where $E^*_{tip} = E_{tip}$ for plane stress and $E^*_{tip} = E_{tip}/(1-\nu^2_{tip})$ for plane strain.

The asymptotic stress and displacement fields Eqs. (10.36) and (10.37) are only valid at points very close to the crack tip as compared with the crack length or any other in-plane characteristic lengths of the cracked body. While gradients of the elastic moduli do not influence the inverse square-root singularity, they may affect the size of the K-dominance zone in which the solution Eq. (10.36) holds. A simple estimate of the effect of material gradation on the size of the K-dominance zone may be made on the basis of Eq. (10.31) and the asymptotic solution Eq. (10.36). For a Mode I crack, at a radial distance r from the crack tip,

$$\frac{\partial^2\phi}{\partial x_\alpha \partial x_\beta} \sim \frac{K_I}{\sqrt{2\pi r}}$$

to within an angular multiplier of order unity. This singularity is due to the first term in Eq. (10.31). Neglecting gradients of Poisson's ratio, the dominance of this first term over the other terms involving modulus gradients in Eq. (10.31) leads to the K-dominance conditions related to material nonhomogeneities [10-7]:

$$\frac{1}{E}\left|\frac{\partial E}{\partial x_\alpha}\right| << \frac{1}{r}, \qquad \frac{1}{E}\left|\frac{\partial^2 E}{\partial x_\alpha \partial x_\beta}\right| << \frac{1}{r^2}. \tag{10.38}$$

This condition shows that the size of the K-dominance zone decreases with increasing magnitude of modulus gradients. The K-dominance zone becomes vanishingly small for a crack located in a nearly sharp interface region where the modulus gradients become extremely steep.

When the modulus gradients are moderate in the crack tip region and a K-dominance zone exists, crack growth can be predicted based on the SIF criterion, that is

$$K_I = K_{Ic}^{tip}$$

where K_{Ic}^{tip} is the fracture toughness value at the crack tip location. Note that for nonhomogenous materials, fracture toughness is generally a function of spatial position, that is, $K_{Ic} = K_{Ic}(x, y)$.

10.2.3 Energy Release Rate

We know from Chapter 4 that for homogeneous elastic materials, the energy release rate is represented by a contour integral—the path-independent J-integral. This section derives the integral representation of energy release rate for nonhomogeneous materials [10-8]. It will be seen that the energy release rate can no longer be represented by a contour integral only. Similar to the approach for homogeneous materials introduced in Chapter 4, we onsider a two-dimensonal nonhomogeneous medium with a crack of length a shown shown in Figure 10.3. The area of the cracked medium is denoted by A_0 and the the boundary is Γ_0. The boundary Γ_0 consists of the outer contour Γ and the crack surfaces Γ_a, that is,

$$\Gamma_0 = \Gamma \cup \Gamma_a$$

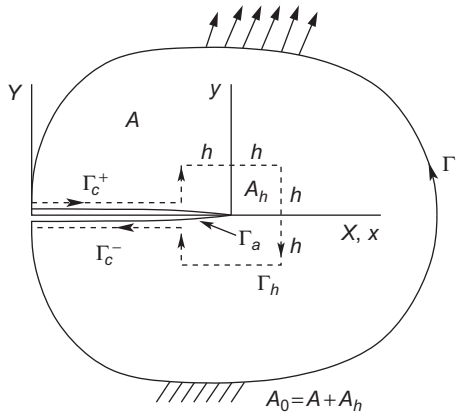

FIGURE 10.3

Contours and coordinate systems in a nonhomogeneous medium with a crack.

The medium is subjected to the prescribed traction T_i along the boundary segment Γ_t and the prescribed displacements on the boundary segment Γ_u. The crack surfaces are along the X-axis and are assumed to be free of traction. The positive contour direction of Γ_0 is defined in that when one travels along it, the domain of interest always lies to the left of the traveler. The potential energy Π of the cracked system per unit thickness can be written as

$$\Pi = \Pi(a) = \iint_{A_0} W dX dY - \int_{\Gamma_t} T_i u_i d\Gamma \tag{10.39}$$

where a is the crack length and (X, Y) is a stationary Cartesian coordinate system. Again, the body forces are absent. For nonhomogeneous materials, the strain energy density W in Eq. (10.39) is an explicit function of spatial position and is given by

$$W = \mu(X, Y)\left[e_{ij}e_{ij} + \frac{\nu(X, Y)}{1 - 2\nu(X, Y)}(e_{kk})^2\right] \tag{10.40}$$

The energy release rate is defined by

$$G = -\frac{d\Pi}{da} = -\frac{d}{da}\iint_{A_0} W dX dY + \frac{d}{da}\int_{\Gamma_t} T_i u_i d\Gamma \tag{10.41}$$

We now consider a small square A_h with the center at the crack tip and boundary Γ_h as shown in Figure 10.3. The region of the cracked body excluding A_h is denoted by A, that is,

$$A_0 = A \cup A_h$$

Because no stress singularity exists in A and along Γ_t, Eq. (10.41) can be written as

$$\begin{aligned} G &= -\frac{d}{da}\left[\iint_{A} W dX dY + \iint_{A_h} W dX dY\right] + \int_{\Gamma_t} T_i \frac{du_i}{da} d\Gamma \\ &= -\iint_{A} \frac{dW}{da} dX dY + \int_{\Gamma_0} T_i \frac{du_i}{da} d\Gamma - \frac{d}{da}\iint_{A_h} W dX dY \end{aligned} \tag{10.42}$$

Here the integration along Γ_t is extended to the entire boundary Γ_0 because $T_i = 0$ on the crack faces Γ_a and $du_i/da = 0$ on Γ_u. By using a local coordinate system (x, y) attached at the crack tip,

$$x = X - a, \quad y = Y$$

$$\frac{d(\,)}{da} = \frac{\partial(\,)}{\partial a} - \frac{\partial(\,)}{\partial x}$$

Equation (10.42) can be written as

$$G = -\iint_A \frac{\partial W}{\partial a} dxdy + \int_{\Gamma_0} T_i \frac{\partial u_i}{\partial a} d\Gamma + \iint_A \frac{\partial W}{\partial x} dxdy - \int_{\Gamma_0} T_i \frac{\partial u_i}{\partial x} d\Gamma - \frac{d}{da} \iint_{A_h} W dXdY \tag{10.43}$$

For nonhomogeneous materials, using the divengence theorem and traction-free conditions along the crack surfaces gives

$$\iint_A \frac{\partial W}{\partial a} dxdy = \int_{\Gamma+\Gamma_h} T_i \frac{\partial u_i}{\partial a} \, d\Gamma + \iint_A \left(\frac{\partial W}{\partial x}\right)_{\text{expl}} dxdy$$

where $(\partial W/\partial x)_{\text{expl}}$ denotes the explicit derivative of W with respect to x, that is,

$$\left(\frac{\partial W}{\partial x}\right)_{\text{expl}} = \frac{\partial W(e_{ij}, x, y)}{\partial x}\Big|_{y=const., e_{ij}=const.}$$

Note that on the crack surface $T_i = dy = 0$. Use of the divergence theorem thus gives

$$\iint_A \frac{\partial W}{\partial x} dA = \int_{\Gamma+\Gamma_h} W n_x d\Gamma = \int_{\Gamma+\Gamma_h} W dy$$

Hence,

$$G = \int_{\Gamma} W dy - \int_{\Gamma} T_i \frac{\partial u_i}{\partial x} d\Gamma - \iint_A \left(\frac{\partial W}{\partial x}\right)_{\text{expl}} dxdy + \int_{\Gamma_h} W dy - \int_{\Gamma_h} T_i \frac{\partial u_i}{\partial a} d\Gamma - \frac{d}{da} \iint_{A_h} W dXdY \tag{10.44}$$

Based on the results in the previous section, the strain energy density function for nonhomogeneous materials has the following universal separable form in the region near the moving crack tip:

$$W = B(a)\widetilde{W}(X - a, Y) = B(a)\widetilde{W}(x, y) \tag{10.45}$$

where $B(a)$ may depend on loading and other factors but not on the local coordinates, and $\widetilde{W}(x, y)$ is a function of local coordinates only. Now assume that A_h is so small

that Eq. (10.45) holds in a region containing A_h. It can be shown that the last three terms on the right-hand side of Eq. (10.44) reduce to

$$-\iint\limits_{A_h}\left(\frac{\partial W}{\partial x}\right)_{\text{expl}} dxdy$$

We thus obtain the expression of energy release rate for nonhomogeneous materials:

$$G=\int\limits_{\Gamma}\left(Wdy-T_i\frac{\partial u_i}{\partial x}d\Gamma\right)-\iint\limits_{A_0}\left(\frac{\partial W}{\partial x}\right)_{\text{expl}} dxdy \tag{10.46}$$

This expression shows that for nonhomogeneous materials, the energy release rate consists of a contour and a domain integral. The domain integral is due to the explicit dependence of strain energy density on the spatial position as shown in Eq. (10.40). The energy release rate in Eq. (10.46) is the path/domain-independent J^*-integral introduced by Eischen [10-6].

Consider a special nonhomgeneous elastic material with an exponentially graded shear modulus μ and constant Poisson's ratio ν:

$$\mu=\mu_0\exp(\beta X),\qquad \nu=\nu_0$$

The strain energy density Eq. (10.40) for this material becomes

$$W=\mu_0\exp(\beta X)\left[e_{ij}e_{ij}+\frac{\nu_0}{1-2\nu_0}(e_{kk})^2\right]$$

The explicit derivative of W with respect to x is

$$\left(\frac{\partial W}{\partial x}\right)_{\text{expl}}=\beta\mu_0\exp(\beta X)\left[e_{ij}e_{ij}+\frac{\nu_0}{1-2\nu_0}(e_{kk})^2\right]=\beta W$$

Note that

$$\iint\limits_{A_0}\beta W dxdy=\frac{\beta}{2}\iint\limits_{A_0}\sigma_{ij}u_{i,j}dxdy=\frac{\beta}{2}\int\limits_{\Gamma+\Gamma_a}\sigma_{ij}u_i n_j d\Gamma=\frac{\beta}{2}\int\limits_{\Gamma}T_i u_i d\Gamma$$

The energy release rate G in Eq. (10.46) now becomes a contour integral:

$$G=\int\limits_{\Gamma}\left(Wdy-T_i\frac{\partial u_i}{\partial x}d\Gamma-\frac{\beta}{2}T_i u_i d\Gamma\right)$$

This is the path-independent J_e-integral presented by Honein and Herrmann [10-9].

10.2.4 Stress Intensity Factors for a Crack in a Graded Interlayer between Two Dissimilar Materials

One of the advantages of graded materials is to eliminate material property mismatch at a sharp interface between two dissimilar materials thereby enhancing the interfacial bonding strength and reducing the thermal residual stresses at the interface. Delale and Erdogan [10-10] considered two dissimilar homogeneous semi-infinite media bonded through a graded interlayer with a crack parallel to the interfaces as shown in Figure 10.4, where h_0 is the thickness of the graded layer, h_1 and h_2 the distances between the crack and the upper and lower interfaces, respectively, and a the half crack length.

Delale and Erdogan [10-10] assumed the following Young's modulus and Poisson's ratio in the graded layer:

$$E = E_0 \exp(\beta y), \quad \nu = \nu_0(1+\gamma y)\exp(\beta y), \quad -h_2 \le y \le h_1, \tag{10.47}$$

where E_0, ν_0, β, and γ are material constants that can be determined using the continuity requirements of material properties across the interfaces between the graded layer and the homogeneous half planes as follows:

$$\begin{aligned} E_0 &= E_1 \exp(-\beta h_1), \quad \beta = \frac{1}{h_0}\ln\frac{E_1}{E_2}, \\ \nu_0 &= \nu_1 \frac{\exp(-\beta h_1)}{1+\gamma h_1}, \quad \gamma = \frac{\nu_1 - \nu_2 \exp(\beta h_0)}{\nu_1 h_2 + \nu_2 h_1 \exp(\beta h_0)}, \end{aligned} \tag{10.48}$$

where E_1 and ν_1 are the Young's modulus and Poisson's ratio of the upper homogeneous half plane ($y \ge h_1$), respectively, and E_2 and ν_2 the material properties of the lower homogeneous half plane ($y \le -h_2$). The function $\nu(y)$ given in

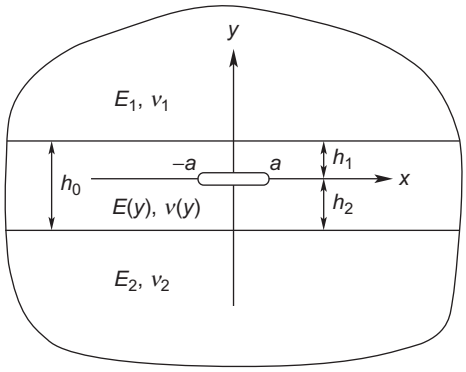

FIGURE 10.4

Two dissimilar homogeneous materials bonded by a graded interlayer with a crack parallel to the interfaces.

Eq. (10.48) should satisfy the physical requirement of $-1 \le \nu \le 0.5$. The governing equation (10.31) in the graded layer now reduces to

$$\nabla^2\nabla^2\phi - 2\beta\frac{\partial}{\partial y}\nabla^2\phi + \beta^2\frac{\partial^2\phi}{\partial y^2} = 0, \quad -h_2 < y < h_1 \tag{10.49}$$

In the homogeneous half planes, the Airy stress function satisfies the biharmonic equation, that is,

$$\nabla^2\nabla^2\phi = 0, \quad y > h_1 \text{ and } y < -h_2$$

Delale and Erdogan [10-10] considered the following material combination: $E_1 = 3 \times 10^4$ ksi = 206.85 GPa, $\nu_1 = 0.3$, and $E_2 = 10^4$ ksi = 68.95 GPa, $\nu_2 = 0.3$. Table 10.1 lists SIFs (normalized by $p_0\sqrt{\pi a}$) for various values of h_1/h_0 and a/h_1 under uniform pressure load p_0 on the crack faces, and Table 10.2 shows the SIFs (normalized by $q_0\sqrt{\pi a}$) under the uniform shearing load q_0 on the crack faces. More detailed results can be found in Delale and Erdogan [10-10]. Unlike the oscillatory nature of stress and displacement fields found in the sharp interface crack problems (Chapter 8), the usual inverse square-root singularity now prevails and the SIF is well defined for the crack in this composite system due to the continuous variations of material properties.

It is seen from the tables that under uniform pressure loading, both the normalized Mode I and Mode II SIFs increase with increasing a/h_1 for a given crack location in the graded layer when $h_1/h_0 \le 0.5$. For a given crack length, the Mode I SIF increases with decreasing h_1/h_0 indicating material gradation effects. The Mode I SIFs are negative under uniform shear loading, indicating crack face contact in the crack tip region only if the shearing load is applied at the crack faces.

Table 10.1 Normalized Stress Intensity Factors under Uniform Crack Face Pressure p_0

h_1/h_0	a/h_1	$K_I/(p_0\sqrt{\pi a})$	$K_{II}/(p_0\sqrt{\pi a})$
0.25	0.1	1.001	0.001
	1.0	1.044	0.051
	8.0	1.159	0.164
0.50	0.1	1.001	0.004
	1.0	1.026	0.092
	8.0	1.046	0.165
0.75	0.1	0.998	0.011
	1.0	0.950	0.098
	8.0	0.915	0.158

Source: Adapted from Delale and Erdogan [10-10].

Table 10.2 Normalized Stress Intensity Factors under Uniform Crack Face Shear q_0

h_1/h_0	a/h_1	$K_I/(q_0\sqrt{\pi a})$	$K_{II}/(q_0\sqrt{\pi a})$
0.25	0.1	−0.001	1.000
	1.0	−0.060	1.011
	8.0	−0.152	1.072
0.50	0.1	−0.004	1.000
	1.0	−0.089	1.002
	8.0	−0.162	1.024
0.75	0.1	−0.011	0.998
	1.0	−0.101	0.973
	8.0	−0.160	0.926

Source: Adapted from Delale and Erdogan [10-10].

10.3 DYNAMIC FRACTURE MECHANICS

Many engineering structures are designed to resist dynamic loads such as explosive loads, wind loads, impact by foreign objects, and so on. The behavior of cracks in a dynamically loaded structure differs from that under quasistatic loads. Moreover, material properties also become rate-dependent when the loading rate is high. Dynamic fracture mechanics deals with crack initiation and propagation in materials and structures when the inertia effects can not be ignored.

Generally speaking, there are two kinds of dynamic fracture problems, that is, stationary cracks under dynamic loading and rapid crack propagation and crack arrest. In this chapter, we introduce some basic concepts and theories of dynamic fracture mechanics in the framework of linear elasticity. The rate effects of constitutive relations of materials thus will not be a concern. However, the rate dependence of dynamic fracture toughness will be included in the fracture criteria.

10.3.1 Basic Equations of Plane Elastodynamics

The basic equations of plane elastodynamics consist of equations of motion,

$$\begin{aligned} \frac{\partial \sigma_{xx}}{\partial x} + \frac{\partial \sigma_{xy}}{\partial y} &= \rho \ddot{u}_x \\ \frac{\partial \sigma_{xy}}{\partial x} + \frac{\partial \sigma_{yy}}{\partial y} &= \rho \ddot{u}_y \end{aligned} \tag{10.50}$$

strain-displacement relations,

$$e_{xx} = \frac{\partial u_x}{\partial x}, \quad e_{yy} = \frac{\partial u_y}{\partial y}, \quad e_{xy} = \frac{1}{2}\left(\frac{\partial u_x}{\partial y} + \frac{\partial u_y}{\partial x}\right) \tag{10.51}$$

and Hooke's law,

$$\begin{aligned}\sigma_{xx} &= \lambda^* \left(e_{xx} + e_{yy}\right) + 2\mu e_{xx} \\ \sigma_{yy} &= \lambda^* \left(e_{xx} + e_{yy}\right) + 2\mu e_{yy} \\ \sigma_{xy} &= 2\mu e_{xy}\end{aligned} \tag{10.52}$$

In these equations, a dot over a quantity denotes its material derivative with respect to time, t is time, ρ is the mass density, λ and μ are Lame constants related to Young's modulus and Poisson's ratio by

$$\lambda = \frac{E\nu}{(1+\nu)(1-2\nu)}, \qquad \mu = \frac{E}{2(1+\nu)} \tag{10.53}$$

and λ^* is given by

$$\lambda^* = \begin{cases} \lambda & \text{for plane strain} \\ \dfrac{2\lambda\mu}{\lambda + 2\mu} & \text{for plane stress} \end{cases} \tag{10.54}$$

The stresses can be expressed in terms of displacements using Hooke's law and strain-displacement relations as follows:

$$\begin{aligned}\sigma_{xx} &= \lambda^* \left(\frac{\partial u_x}{\partial x} + \frac{\partial u_y}{\partial y}\right) + 2\mu \frac{\partial u_x}{\partial x} \\ \sigma_{yy} &= \lambda^* \left(\frac{\partial u_x}{\partial x} + \frac{\partial u_y}{\partial y}\right) + 2\mu \frac{\partial u_y}{\partial y} \\ \sigma_{xy} &= \mu \left(\frac{\partial u_x}{\partial y} + \frac{\partial u_y}{\partial x}\right)\end{aligned} \tag{10.55}$$

Substituting these stresses into the equations of motion yields the following governing equations of displacements:

$$\begin{aligned}\mu \nabla^2 u_x + (\lambda^* + \mu) \frac{\partial}{\partial x} \left(\frac{\partial u_x}{\partial x} + \frac{\partial u_y}{\partial y}\right) &= \rho \ddot{u}_x \\ \mu \nabla^2 u_y + (\lambda^* + \mu) \frac{\partial}{\partial y} \left(\frac{\partial u_x}{\partial x} + \frac{\partial u_y}{\partial y}\right) &= \rho \ddot{u}_y\end{aligned} \tag{10.56}$$

The basic equations here can be converted to the standard wave equations using the following displacement potentials φ and ψ:

$$u_x = \frac{\partial \varphi}{\partial x} + \frac{\partial \psi}{\partial y}, \qquad u_y = \frac{\partial \varphi}{\partial y} - \frac{\partial \psi}{\partial x} \tag{10.57}$$

Substituting this equation into Eq. (10.56) leads to the following wave equations for the potentials φ and ψ:

$$\nabla^2\varphi = \frac{1}{c_1^2}\ddot{\varphi}, \qquad \nabla^2\psi = \frac{1}{c_2^2}\ddot{\psi} \tag{10.58}$$

where ∇^2 is the Laplace operator

$$\nabla^2 = \frac{\partial^2}{\partial x^2} + \frac{\partial^2}{\partial y^2}$$

and c_1 and c_2 are given by

$$c_1 = \sqrt{\frac{\lambda^* + 2\mu}{\rho}}, \qquad c_2 = \sqrt{\frac{\mu}{\rho}} \tag{10.59}$$

c_1 and c_2 are the dilatational and shear wave speeds of the medium, respectively.

10.3.2 Stationary Cracks under Dymanic Loading

To study crack initiation under dynamic loading, we first analyze the stress and displacement fields near a stationary crack tip. Because the displacements are finite, their derivatives with respect to time are also bounded for stationary cracks. In the mean time, the stresses and their derivatives with respect to spatial coordinates are expected to be singular at the crack tip. The left side terms in the equations of motion (10.50) thus dominate the inertial terms on the right side. Hence in the near-tip region, the forms of the equations of motion reduce to those of equilibrium equations as follows:

$$\begin{aligned} \frac{\partial \sigma_{xx}}{\partial x} + \frac{\partial \sigma_{xy}}{\partial y} &= 0 \\ \frac{\partial \sigma_{xy}}{\partial x} + \frac{\partial \sigma_{yy}}{\partial y} &= 0 \end{aligned} \tag{10.60}$$

Because the material is still assumed to be linear elastic, the stress and displacement fields near the crack tip will have the same forms as those in the quasistatic linear elastic fracture mechanics introduced in Chapter 3. Hence, the inertial effect does not alter the singularity structure of stress and displacement fields near the tip of a stationary crack under dynamic loading. The crack tip stress and displacement fields are thus given by

$$\begin{aligned} \sigma_{xx} = {} & \frac{K_I(t)}{\sqrt{2\pi r}} \cos\frac{1}{2}\theta \left(1 - \sin\frac{1}{2}\theta \sin\frac{3}{2}\theta\right) \\ & - \frac{K_{II}(t)}{\sqrt{2\pi r}} \sin\frac{1}{2}\theta \left(2 + \cos\frac{\theta}{2}\cos\frac{3\theta}{2}\right) \end{aligned}$$

$$\sigma_{yy} = \frac{K_I(t)}{\sqrt{2\pi r}} \cos\frac{1}{2}\theta \left(1 + \sin\frac{1}{2}\theta \sin\frac{3}{2}\theta\right) + \frac{K_{II}(t)}{\sqrt{2\pi r}} \sin\frac{\theta}{2} \cos\frac{\theta}{2} \cos\frac{3}{2}\theta$$

$$\sigma_{xy} = \frac{K_I(t)}{\sqrt{2\pi r}} \sin\frac{1}{2}\theta \cos\frac{1}{2}\theta \cos\frac{3}{2}\theta + \frac{K_{II}(t)}{\sqrt{2\pi r}} \cos\frac{1}{2}\theta \left(1 - \sin\frac{1}{2}\theta \sin\frac{3}{2}\theta\right) \tag{10.61}$$

and

$$u_x = \frac{K_I(t)}{8\mu\pi}\sqrt{2\pi r}\left[(2\kappa - 1)\cos\frac{\theta}{2} - \cos\frac{3\theta}{2}\right] + \frac{K_{II}(t)}{8\mu\pi}\sqrt{2\pi r}\left[(2\kappa + 3)\sin\frac{\theta}{2} + \sin\frac{3\theta}{2}\right]$$

$$u_y = \frac{K_I(t)}{8\mu\pi}\sqrt{2\pi r}\left[(2\kappa + 1)\sin\frac{\theta}{2} - \sin\frac{3\theta}{2}\right] - \frac{K_{II}(t)}{8\mu\pi}\sqrt{2\pi r}\left[(2\kappa - 3)\cos\frac{\theta}{2} + \cos\frac{3\theta}{2}\right] \tag{10.62}$$

where $K_I(t)$ and $K_{II}(t)$ are the dynamic stress intensity factors (DSIFs) and (r,θ) are the polar coordinates centered at the crack tip with crack surfaces at $\theta = \pm\pi$. $K_I(t)$ and $K_{II}(t)$ depend not only on the magnitude of the dynamic load and crack configuration, but also time t. In general, the peak values of the DSIFs for a given crack geometry are higher than the corresponding SIFs under the quasistatic loading of the same magnitude.

The monographs by Sih [10-11] and Freund [10-12] provide the DSIF solutions for various cracks under crack face impact loads as well as wave loads. Closed-form solutions of DSIFs are available for only a few problems of dynamically loaded stationary cracks. Maue [10-13] considered a semi-infinite crack subjected to a sudden crack face pressure σ_0 at time $t = 0$ and gave the closed-form DSIF as follows:

$$K_I(t) = \frac{2\sqrt{2}}{\pi}\frac{c_R}{c_1}\sigma_0\sqrt{\pi c_1 t} \tag{10.63}$$

where c_R is the Rayleigh surface wave speed, which is the smallest real root of the following equation:

$$\left(2 - \frac{c_R^2}{c_2^2}\right)^2 - 4\left(1 - \frac{c_R^2}{c_1^2}\right)^{1/2}\left(1 - \frac{c_R^2}{c_2^2}\right)^{1/2} = 0 \tag{10.64}$$

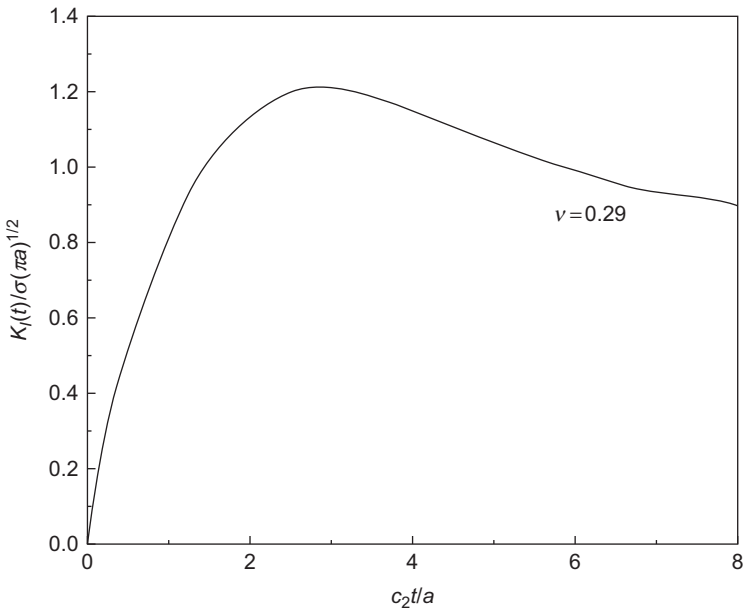

FIGURE 10.5

Mode I dynamic stress intensity factor versus nondimensional time for a central crack of length $2a$ in an infinite plate subjected to sudden crack face pressure σ (adapted from Sih et al. [10-14]).

Note that $c_R < c_2 < c_1$. Equation (10.63) shows that the DSIF depends on both dilatational and Rayleigh surface wave speeds. Moreover, the DSIF is zero at the start of loading and increases monotonically with time.

Sih et al. [10-14] investigated a central crack of length $2a$ in an infinite plate subjected to sudden crack face pressure σ at time $t = 0$. They computed the DSIF using an integral transform/integral equation approach. The numerical result is shown in Figure 10.5.

It is seen that the DSIF initially increases with time, reaches the peak value at about $c_2t/a = 3.0$, and then decreases with time. The peak DSIF is approximately 20% percent higher than the corresponding quasistatic SIF of $\sigma\sqrt{\pi a}$. The DSIF approaches the quasistatic SIF in the steady state limit ($t \to \infty$).

In general, DSIFs have to be obtained using numerical methods, for example, the finite element method. The DSIF versus time response can be quite complicated due to wave reflections at the crack surface and structural boundaries.

The crack tip stress field Eq. (10.61) indicates that similar to the quasistatic cracks, the DSIFs determine the intensity of the singular stresses around the crack tip. Crack initiation thus can be predicted based on the SIF criterion, that is, crack initiation

occurs when the DSIF reaches the dynamic fracture toughness of the material K_{Id}:

$$K_I(t) = K_{Id} \tag{10.65}$$

This fracture criterion is applicable to brittle materials such as engineering ceramics and rocks, as well as metals when small-scale yielding conditions prevail.

We know from Chapters 3 and 6 that crack tip plastic energy dissipation significantly contributes to the fracture toughness of metals. It is also known that the plastic properties of metals are rate-dependent. Metals usually become less ductile at higher loading rates, that is, the yield strength increases with increasing loading rate whereas the ductility decreases. The dynamic fracture toughness K_{Id} thus tends to decrease with increasing loading rate as the crack tip plastic deformation is supressed at higher loading rates. However, the dependence of K_{Id} on loading rate can be complex as high strain rates in the crack tip region cause temperature variation, which in turn also influences the material's constitutive behavior. K_{Id} reduces to K_{Ic} at vanishing loading rate.

10.3.3 Dynamic Crack Propagation

In a linear elastic material, a crack will propagate unstably once it has initiated. The crack propagation will lead to dynamic failure of the material unless it is arrested. Studies of the stress and displacement fields near a propagating crack tip usually employ a moving coordinate system (x_1, y_1) centered at the crack tip, as shown in Figure 10.6, where (x, y) is a fixed coordinate system and $a(t)$ is current crack propagation distance. The two systems are related by

$$x_1 = x - a(t), \quad y_1 = y \tag{10.66}$$

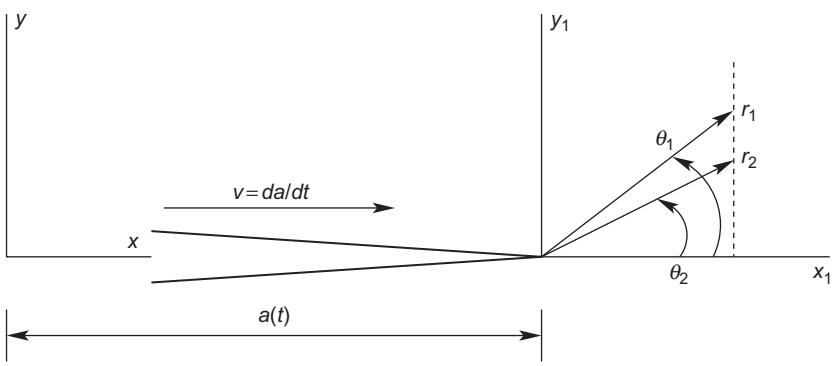

FIGURE 10.6

Coordinate systems attached to the moving crack tip.

The material derivative in the moving coordinates becomes

$$\frac{d(\,)}{dt} = \frac{\partial(\,)}{\partial t} - V\frac{\partial(\,)}{\partial x_1} \tag{10.67}$$

where $V = \dot{a} = da/dt$ is the crack propagation speed.

Using the material derivative Eq. (10.67) and coordinate transformation Eq. (10.66), the wave equations (10.58) in the moving coordinates can be written as follows:

$$\frac{\partial^2\varphi}{\partial x_1^2} + \frac{\partial^2\varphi}{\partial y_1^2} = \frac{1}{c_1^2}\left(\frac{\partial^2\varphi}{\partial t^2} - 2V\frac{\partial^2\varphi}{\partial x_1\partial t} - \dot{V}\frac{\partial\varphi}{\partial x_1} + V^2\frac{\partial^2\varphi}{\partial x_1^2}\right)$$
$$\frac{\partial^2\psi}{\partial x_1^2} + \frac{\partial^2\psi}{\partial y_1^2} = \frac{1}{c_2^2}\left(\frac{\partial^2\psi}{\partial t^2} - 2V\frac{\partial^2\psi}{\partial x_1\partial t} - \dot{V}\frac{\partial\psi}{\partial x_1} + V^2\frac{\partial^2\psi}{\partial x_1^2}\right)$$

These equations can be rewritten as

$$\begin{aligned}\alpha_1^2\frac{\partial^2\varphi}{\partial x_1^2} + \frac{\partial^2\varphi}{\partial y_1^2} &= \frac{1}{c_1^2}\left(\frac{\partial^2\varphi}{\partial t^2} - 2V\frac{\partial^2\varphi}{\partial x_1\partial t} - \dot{V}\frac{\partial\varphi}{\partial x_1}\right)\\ \alpha_2^2\frac{\partial^2\psi}{\partial x_1^2} + \frac{\partial^2\psi}{\partial y_1^2} &= \frac{1}{c_2^2}\left(\frac{\partial^2\psi}{\partial t^2} - 2V\frac{\partial^2\psi}{\partial x_1\partial t} - \dot{V}\frac{\partial\psi}{\partial x_1}\right)\end{aligned} \tag{10.68}$$

where α_1 and α_2 are given by

$$\alpha_1 = \sqrt{1 - \left(\frac{V}{c_1}\right)^2}, \qquad \alpha_2 = \sqrt{1 - \left(\frac{V}{c_2}\right)^2} \tag{10.69}$$

Note that $\alpha_1 > \alpha_2$ as $c_1 > c_2$. When the stresses are singular at the moving crack tip, the terms on the left side of Eq. (10.68) dominate because the terms on the right side have weaker singularities. In the crack tip region, Eq. (10.68) reduce to

$$\begin{aligned}\alpha_1^2\frac{\partial^2\varphi}{\partial x_1^2} + \frac{\partial^2\varphi}{\partial y_1^2} &= 0\\ \alpha_2^2\frac{\partial^2\psi}{\partial x_1^2} + \frac{\partial^2\psi}{\partial y_1^2} &= 0\end{aligned} \tag{10.70}$$

The preceding equations are essentially Laplace equations in the $(x_1, \alpha_1 y_1)$ and $(x_1, \alpha_2 y_1)$ systems.

Introduce two polar coordinate systems, (r_1, θ_1) and (r_2, θ_2), at the moving crack tip as shown in Figure 10.6:

$$\begin{aligned}x_1 &= r_1\cos\theta_1, \qquad y_1 = \frac{r_1}{\alpha_1}\sin\theta_1\\ x_1 &= r_2\cos\theta_2, \qquad y_1 = \frac{r_2}{\alpha_2}\sin\theta_2\end{aligned} \tag{10.71}$$

or inversely:

$$\begin{aligned} r_1 &= \sqrt{x_1^2 + (\alpha_1 y_1)^2}, \qquad \theta_1 = \tan^{-1}\left(\frac{\alpha_1 y_1}{x_1}\right) \\ r_2 &= \sqrt{x_1^2 + (\alpha_2 y_1)^2}, \qquad \theta_2 = \tan^{-1}\left(\frac{\alpha_2 y_1}{x_1}\right) \end{aligned} \tag{10.72}$$

It follows from these two equations that

$$\begin{aligned} \frac{\partial r_1}{\partial x_1} &= \frac{x_1}{r_1} = \cos\theta_1, \qquad \frac{\partial r_1}{\partial y_1} = \frac{\alpha_1^2 y_1}{r_1} = \alpha_1 \sin\theta_1 \\ \frac{\partial \theta_1}{\partial x_1} &= -\frac{\alpha_1 y_1}{r_1^2} = -\frac{\sin\theta_1}{r_1}, \qquad \frac{\partial \theta_1}{\partial y_1} = \frac{\alpha_1 x_1}{r_1^2} = \alpha_1 \frac{\cos\theta_1}{r_1} \end{aligned} \tag{10.73}$$

$$\begin{aligned} \frac{\partial r_2}{\partial x_1} &= \frac{x_1}{r_2} = \cos\theta_2, \qquad \frac{\partial r_2}{\partial y_1} = \frac{\alpha_2^2 y_1}{r_2} = \alpha_2 \sin\theta_2 \\ \frac{\partial \theta_2}{\partial x_1} &= -\frac{\alpha_2 y_1}{r_2^2} = -\frac{\sin\theta_2}{r_2}, \qquad \frac{\partial \theta_2}{\partial y_1} = \frac{\alpha_2 x_1}{r_2^2} = \alpha_2 \frac{\cos\theta_2}{r_2} \end{aligned} \tag{10.74}$$

Thus,

$$\begin{aligned} \frac{\partial(\,)}{\partial x_1} &= \frac{\partial(\,)}{\partial r_1}\cos\theta_1 - \frac{\partial(\,)}{\partial \theta_1}\frac{\sin\theta_1}{r_1} \\ \frac{\partial(\,)}{\partial y_1} &= \frac{\partial(\,)}{\partial r_1}\alpha_1 \sin\theta_1 + \frac{\partial(\,)}{\partial \theta_1}\alpha_1 \frac{\cos\theta_1}{r_1} \end{aligned} \tag{10.75}$$

in the (r_1, θ_1) system, and

$$\begin{aligned} \frac{\partial(\,)}{\partial x_1} &= \frac{\partial(\,)}{\partial r_2}\cos\theta_2 - \frac{\partial(\,)}{\partial \theta_2}\frac{\sin\theta_2}{r_2} \\ \frac{\partial(\,)}{\partial y_1} &= \frac{\partial(\,)}{\partial r_2}\alpha_2 \sin\theta_2 + \frac{\partial(\,)}{\partial \theta_2}\alpha_2 \frac{\cos\theta_2}{r_2} \end{aligned} \tag{10.76}$$

in the (r_2, θ_2) system. Since $\varphi = \varphi(r_1, \theta_1)$ and $\psi = \psi(r_2, \theta_2)$, Eq. (10.70) can be written in the moving polar coordinates as follows:

$$\begin{aligned} \frac{\partial^2 \varphi}{\partial r_1^2} + \frac{1}{r_1}\frac{\partial \varphi}{\partial r_1} + \frac{1}{r_1^2}\frac{\partial^2 \varphi}{\partial \theta_1^2} &= 0 \\ \frac{\partial^2 \psi}{\partial r_2^2} + \frac{1}{r_2}\frac{\partial \psi}{\partial r_2} + \frac{1}{r_2^2}\frac{\partial^2 \psi}{\partial \theta_2^2} &= 0 \end{aligned} \tag{10.77}$$

These are Laplace equations in the polar (r_1, θ_1) and (r_2, θ_2) coordinate systems, respectively.

To obtain the asymptotic singular stresses at the moving crack tip, the displacement potential functions are assumed to have the following form:

$$\begin{aligned} \varphi &= r_1^s \widetilde{\varphi}(\theta_1), \qquad r_1 \to 0 \\ \psi &= r_2^s \widetilde{\psi}(\theta_2), \qquad r_2 \to 0 \end{aligned} \tag{10.78}$$

where s is the eigenvalue to be determined by the boundary conditions. Substituting these potentials into Eq. (10.77), we have

$$\frac{d^2\widetilde{\varphi}}{d\theta_1^2} + s^2\widetilde{\varphi} = 0$$
$$\frac{d^2\widetilde{\psi}}{d\theta_2^2} + s^2\widetilde{\psi} = 0$$

The general solutions of these equations are

$$\widetilde{\varphi} = C_1\cos(s\theta_1) + C_3\sin(s\theta_1)$$
$$\widetilde{\psi} = C_4\cos(s\theta_2) + C_2\sin(s\theta_2)$$

where C_i $(i = 1,2,3,4)$ are constants. In the following we consider Mode I crack propagation only. Mode I symmetry consideration gives $C_3 = C_4 = 0$. Hence, $\widetilde{\varphi}$ and $\widetilde{\psi}$ reduce to

$$\widetilde{\varphi} = C_1\cos(s\theta_1)$$
$$\widetilde{\psi} = C_2\sin(s\theta_2)$$

Substituting these expressions into Eq. (10.78), and using the relations Eqs. (10.57), (10.55), and (10.73) through (10.76), we obtain the following dominant asymptotic expressions for the displacement potentials, displacements, and stresses at the moving crack tip ($r_1 \to 0$, $r_2 \to 0$):

$$\begin{aligned} \varphi &= C_1 r_1^s \cos(s\theta_1) \\ \psi &= C_2 r_2^s \sin(s\theta_2) \end{aligned} \tag{10.79}$$

$$\begin{aligned} u_x &= sC_1 r_1^{s-1}\cos(s-1)\theta_1 + \alpha_2 sC_2 r_2^{s-1}\cos(s-1)\theta_2 \\ u_y &= -\alpha_1 sC_1 r_1^{s-1}\sin(s-1)\theta_1 - sC_2 r_2^{s-1}\sin(s-1)\theta_2 \end{aligned} \tag{10.80}$$

and

$$\begin{aligned} \sigma_{xx} &= \rho c_2^2\big(s^2 - s\big)\big(1 + 2\alpha_1^2 - \alpha_2^2\big)C_1 r_1^{s-2}\cos(s-2)\theta_1 \\ &\quad + 2\rho c_2^2\big(s^2 - s\big)\alpha_2 C_2 r_2^{s-2}\cos(s-2)\theta_2 \\ \sigma_{yy} &= -\rho c_2^2\big(s^2 - s\big)\big(1 + \alpha_2^2\big)C_1 r_1^{s-2}\cos(s-2)\theta_1 \end{aligned}$$

$$\begin{aligned}\sigma_{xy} = &-2\rho c_2^2\left(s^2-s\right)\alpha_2 C_2 r_2^{s-2}\cos(s-2)\theta_2 \\ &-2\rho c_2^2\left(s^2-s\right)\alpha_1 C_1 r_1^{s-2}\sin(s-2)\theta_1 \\ &-\rho c_2^2\left(s^2-s\right)\left(1+\alpha_2^2\right)C_2 r_2^{s-2}\sin(s-2)\theta_2 \end{aligned} \tag{10.81}$$

The preceding stresses and displacements already satisfy the symmetry conditions along the crack line, that is,

$$\sigma_{xy} = u_y = 0, \qquad \theta_1 = \theta_2 = 0$$

The crack surface boundary conditions for the analysis of crack tip asymptotic solutions are

$$\sigma_{xy} = \sigma_{yy} = 0, \qquad \theta_1 = \theta_2 = \pi \tag{10.82}$$

Substituting the stress expressions in Eq. (10.81) into the boundary conditions in Eq. (10.82) yields two equations satisfied by constants C_1 and C_2 as follows ($r_1 = r_2$ at $\theta_1 = \theta_2 = \pi$):

$$\begin{aligned}&-2\rho c_2^2\left(s^2-s\right)\alpha_1 C_1\sin(s-2)\pi - \rho c_2^2\left(s^2-s\right)\left(1+\alpha_2^2\right)C_2\sin(s-2)\pi = 0 \\ &-\rho c_2^2\left(s^2-s\right)\left(1+\alpha_2^2\right)C_1\cos(s-2)\pi - 2\rho c_2^2\left(s^2-s\right)\alpha_2 C_2\cos(s-2)\pi = 0\end{aligned} \tag{10.83}$$

For the nontrivial solutions to exist, the determinant of the equation systems here must be zero, that is,

$$\begin{aligned}&\rho c_2^2\left(s^2-s\right)\left[4\alpha_1\alpha_2 - \left(1+\alpha_2^2\right)^2\right]\cos[(s-2)\pi]\sin[(s-2)\pi] \\ &= \frac{1}{2}\rho c_2^2\left(s^2-s\right)\left[4\alpha_1\alpha_2 - \left(1+\alpha_2^2\right)^2\right]\sin[2(s-2)\pi] = 0\end{aligned} \tag{10.84}$$

Equation (10.84) is the characteristic equation for determination of the eigenvalue s. Its root that leads to both finite strain energy and stress singularity is

$$s = 3/2$$

There is only one independent equation in Eq. (10.83), which gives the relation between constants C_1 and C_2 as follows:

$$C_2 = -\frac{2\alpha_1}{1+\alpha_2^2}C_1$$

The constants C_1 can be related to the Mode I dynamic SIF $K_I(t)$:

$$C_1 = \frac{4\left(1+\alpha_2^2\right)}{\mu\left[4\alpha_1\alpha_2 - \left(1+\alpha_2^2\right)^2\right]}\frac{K_I(t)}{3\sqrt{2\pi}}$$

with $K_I(t)$ defined by

$$K_I(t) = \lim_{r_1\to 0}\sqrt{2\pi r_1}\,\sigma_{yy}(r_1, r_2, \theta_1, \theta_2)|_{\theta_1=\theta_2=0, r_1=r_2}$$

The crack tip dominant stress and displacement fields can thus be written in the following form:

$$\sigma_{xx} = \frac{K_I(t)}{\sqrt{2\pi}} \frac{1+\alpha_2^2}{4\alpha_1\alpha_2 - (1+\alpha_2^2)^2} \left[\frac{1+2\alpha_1^2-\alpha_2^2}{\sqrt{r_1}} \cos\frac{\theta_1}{2} - \frac{4\alpha_1\alpha_2}{(1+\alpha_2^2)\sqrt{r_2}} \cos\frac{\theta_2}{2} \right]$$

$$\sigma_{yy} = \frac{K_I(t)}{\sqrt{2\pi}} \frac{1+\alpha_2^2}{4\alpha_1\alpha_2 - (1+\alpha_2^2)^2} \left[-\frac{1+\alpha_2^2}{\sqrt{r_1}} \cos\frac{\theta_1}{2} + \frac{4\alpha_1\alpha_2}{(1+\alpha_2^2)\sqrt{r_2}} \cos\frac{\theta_2}{2} \right]$$

$$\sigma_{xy} = \frac{K_I(t)}{\sqrt{2\pi}} \frac{2\alpha_1(1+\alpha_2^2)}{4\alpha_1\alpha_2 - (1+\alpha_2^2)^2} \left[\frac{1}{\sqrt{r_1}} \sin\frac{\theta_1}{2} - \frac{1}{\sqrt{r_2}} \sin\frac{\theta_2}{2} \right] \tag{10.85}$$

$$u_x = \frac{K_I(t)}{\sqrt{2\pi}} \frac{2(1+\alpha_2^2)}{\mu\left[4\alpha_1\alpha_2 - (1+\alpha_2^2)^2\right]} \left[\sqrt{r_1}\cos\frac{\theta_1}{2} - \frac{2\alpha_1\alpha_2}{(1+\alpha_2^2)}\sqrt{r_2}\cos\frac{\theta_2}{2} \right]$$

$$u_y = \frac{K_I(t)}{\sqrt{2\pi}} \frac{2(1+\alpha_2^2)}{\mu\left[4\alpha_1\alpha_2 - (1+\alpha_2^2)^2\right]} \left[-\alpha_1\sqrt{r_1}\sin\frac{\theta_1}{2} + \frac{2\alpha_1}{(1+\alpha_2^2)}\sqrt{r_2}\sin\frac{\theta_2}{2} \right] \tag{10.86}$$

The crack tip dominant velocity field can also be obtained by using

$$\frac{d(\,)}{dt} = -V\frac{\partial(\,)}{\partial x_1}, \qquad r_1, r_2 \to 0,$$

and the result is

$$\dot{u}_x = -\frac{VK_I(t)}{\sqrt{2\pi}} \frac{(1+\alpha_2^2)}{\mu\left[4\alpha_1\alpha_2 - (1+\alpha_2^2)^2\right]} \left[\frac{1}{\sqrt{r_1}}\cos\frac{\theta_1}{2} - \frac{2\alpha_1\alpha_2}{(1+\alpha_2^2)}\frac{1}{\sqrt{r_2}}\cos\frac{\theta_2}{2} \right]$$

$$\dot{u}_y = -\frac{VK_I(t)}{\sqrt{2\pi}} \frac{(1+\alpha_2^2)}{\mu\left[4\alpha_1\alpha_2 - (1+\alpha_2^2)^2\right]} \left[\frac{\alpha_1}{\sqrt{r_1}}\sin\frac{\theta_1}{2} - \frac{2\alpha_1}{(1+\alpha_2^2)}\frac{1}{\sqrt{r_2}}\sin\frac{\theta_2}{2} \right] \tag{10.87}$$

It can be seen that the velocity field has an inverse square root singlarity at the moving crack tip. The stress and displacement fields in Eq. (10.87) under constant crack propagation speed were derived by Rice [10-15]. Freund and Clifton [10-16] and Nielson [10-17] later showed that the results are also valid when the propagation speed varies with time.

Equations (10.85) and (10.86) show that the stresses at a propagating crack tip still have the inverse square singularity. The angular distributions of the stresses and displacements, however, depend on the crack propagation speed. It is interesting to

look at the stress distributions along the crack line ($\theta_1 = \theta_2 = 0$, $r_1 = r_2 = x_1 > 0$). It follows from Eq. (10.85) that

$$\sigma_{xx}|_{\theta_1=\theta_2=0} = \frac{K_I(t)}{\sqrt{2\pi x_1}} \frac{\left(1+\alpha_2^2\right)\left(1+2\alpha_1^2-\alpha_2^2\right)-4\alpha_1\alpha_2}{4\alpha_1\alpha_2-\left(1+\alpha_2^2\right)^2}$$

$$\sigma_{yy}|_{\theta_1=\theta_2=0} = \frac{K_I(t)}{\sqrt{2\pi x_1}}$$

The ratio of σ_{yy} to σ_{xx} at the crack line is

$$\left(\frac{\sigma_{yy}}{\sigma_{xx}}\right)_{\theta_1=\theta_2=0} = \frac{4\alpha_1\alpha_2-\left(1+\alpha_2^2\right)^2}{\left(1+\alpha_2^2\right)\left(1+2\alpha_1^2-\alpha_2^2\right)-4\alpha_1\alpha_2} \tag{10.88}$$

This ratio represents the stress triaxiality ahead of the propagating crack. This ratio is unity for stationary cracks. For rapidly propagating cracks, the ratio varies with the crack speed.

Figure 10.7 schematically shows the variation of the stress ratio versus the nondimensional crack propagation speed V/c_R. It is seen that the stress ratio approaches unity when the crack propagation speed goes to zero, consistent with the stationary crack result. The ratio decreases monotonically with increasing crack speed and approaches zero when the crack speed reaches the Rayleigh surface wave speed. In fracture mechanics, we know that the fracture toughness increases with decreasing triaxiality of the stress field. Equation (10.88) and Figure 10.7 imply that dynamic fracture toughness will increase with increasing crack propagation speed due to the stress ratio effect.

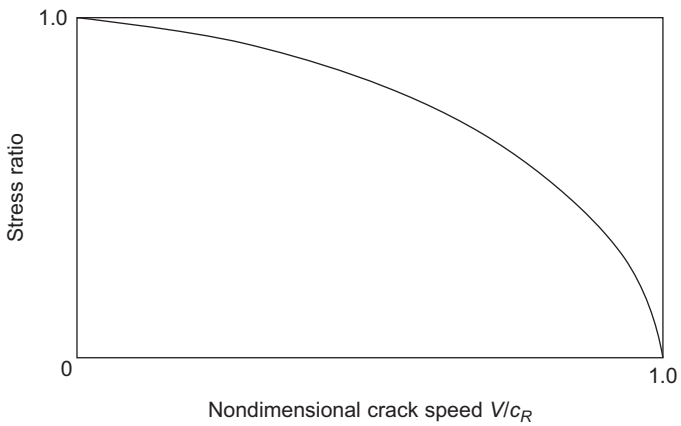

FIGURE 10.7

Stress ratio versus crack propagation speed ahead of the crack.

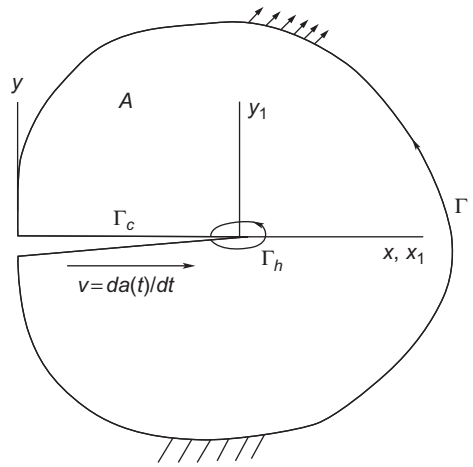

FIGURE 10.8

Dynamic crack propagation and the contours around the moving crack tip.

It is known from Chapter 4 that energy release rate is an important concept in fracture mechanics. To introduce the dynamic energy release rate for a rapidly propagating crack, we consider the flux of energy, F, into the crack tip region through a vanishingly small contour Γ_h around the moving crack tip as shown in Figure 10.8, where Γ is the outer boundary of the cracked body and A is the area bounded by Γ, Γ_h, and the crack faces Γ_c between Γ and Γ_h. The medium is subjected to the prescribed traction T_i along the boundary segment Γ_t and the prescribed displacements on the boundary segment Γ_u. Moreover, the small contour Γ_h is fixed relative to, and moves with the crack tip. Clearly the energy flux F equals the rate of work done by the traction on Γ_t less the rates of increases in the strain energy and kinetic energy, that is,

$$F = \int_{\Gamma_t} T_i \dot{u}_i d\Gamma - \lim_{\Gamma_h \to 0} \frac{d}{dt} \iint_A W dA - \lim_{\Gamma_h \to 0} \frac{d}{dt} \iint_A \frac{1}{2} \rho \dot{u}_i \dot{u}_i dA \tag{10.89}$$

Using the transport theorem, we have

$$\frac{d}{dt} \iint_A W dA = \iint_A \dot{W} dA - \int_{\Gamma_h} W V n_1 d\Gamma$$

$$\frac{d}{dt} \iint_A \frac{1}{2} \rho \dot{u}_i \dot{u}_i dA = \iint_A \rho \ddot{u}_i \dot{u}_i dA - \int_{\Gamma_h} \frac{1}{2} \rho \dot{u}_i \dot{u}_i V n_1 d\Gamma$$

where n_1 is the x-component of the outward unit normal to Γ_h. Substituting these equations in (10.89), we have

$$F = \int_{\Gamma} T_i \dot{u}_i d\Gamma + \lim_{\Gamma_h \to 0} \int_{\Gamma_h} \left(W + \frac{1}{2} \rho \dot{u}_i \dot{u}_i \right) V n_1 d\Gamma - \lim_{\Gamma_h \to 0} \iint_{A} \left(\dot{W} + \rho \ddot{u}_i \dot{u}_i \right) dA \tag{10.90}$$

where the integral along Γ_t has been extended to Γ because $\dot{u}_i$ is zero along Γ_u. Using the definition of W and the equations of motion, we know

$$\dot{W} = \sigma_{ij} \dot{e}_{ij} = \sigma_{ij} \dot{u}_{i,j}$$
$$\sigma_{ij} \dot{u}_{i,j} = \left(\sigma_{ij} \dot{u}_i \right)_{,j} - \sigma_{ij,j} \dot{u}_i = \left(\sigma_{ij} \dot{u}_i \right)_{,j} - \rho \ddot{u}_i \dot{u}_i$$

Use of these relations in the area integral on the right side of Eq. (10.90) and application of the divergence theorem yield

$$\iint_{A} \left(\dot{W} + \rho \ddot{u}_i \dot{u}_i \right) dA = \iint_{A} \left(\sigma_{ij} \dot{u}_i \right)_{,j} dA = \int_{\Gamma + \Gamma_c - \Gamma_h} T_i \dot{u}_i d\Gamma = \int_{\Gamma - \Gamma_h} T_i \dot{u}_i d\Gamma$$

Substituting this into Eq. (10.90), we obtain the energy flux as follows:

$$F = \lim_{\Gamma_h \to 0} \int_{\Gamma_h} \left[\left(W + \frac{1}{2} \rho \dot{u}_i \dot{u}_i \right) V n_1 + T_i \dot{u}_i \right] d\Gamma \tag{10.91}$$

The energy release rate is clearly F/V as $V = da/dt$, and is given by

$$G = \frac{F}{V} = \lim_{\Gamma_h \to 0} \frac{1}{V} \int_{\Gamma_h} \left[\left(W + \frac{1}{2} \rho \dot{u}_i \dot{u}_i \right) V n_1 + T_i \dot{u}_i \right] d\Gamma \tag{10.92}$$

Under steady state conditions, V is a constant and the material derivative in Eq. (10.67) reduces to

$$\frac{d(\,)}{dt} = -V \frac{\partial(\,)}{\partial x_1}$$

The energy release rate Eq. (10.92) becomes

$$G = \lim_{\Gamma_h \to 0} \int_{\Gamma_h} \left[\left(W + \frac{1}{2} \rho V^2 \frac{\partial u_i}{\partial x_1} \frac{\partial u_i}{\partial x_1} \right) n_1 - T_i \frac{\partial u_i}{\partial x_1} \right] d\Gamma \tag{10.93}$$

It can be shown (Atkinson and Eshelby [10-25]) that this integral is a path-independent integral for any contour around the crack tip, beginning at the lower crack surface and ending on the upper crack surface.

Similar to quasistatic cracks, there is a relationship between the DSIF and the dynamic energy release rate G. For plane strain, the relation was obtained by Freund [10-18] and Nilsson [10-19] as follows:

$$G_I(t) = \frac{1-\nu^2}{E} A(V) K_I^2(t) \tag{10.94}$$

where the dynamic factor $A(V)$ is given by

$$A(V) = \frac{1}{1-\nu} \frac{\alpha_1 \left(1-\alpha_2^2\right)}{4\alpha_1\alpha_2 - (1+\alpha_2^2)^2}$$

Figure 10.9 schmeatically shows the variation of factor $A(V)$ with nondimensional crack speed V/c_R. It is seen that $A(V)$ goes to unity in the limit of zero crack speed. The dynamic relation Eq. (10.94) thus reduces to that in the quasistatic fracture mechanics. $A(V)$ increases monotonically with crack speed and goes to infinity when the crack speed approaches the Rayleigh wave speed implying that the maximum crack propagation speed for Mode I cracks is the Rayleigh surface wave speed.

Equation (10.85) indicates that the DSIF is the governing parameter of the crack tip singular stress field. Hence, continuous rapid crack propagation occurs when the DSIF equals its critical value, or fracture propagation toughness, K_{ID}:

$$K_I(t) = K_{ID}(V) \tag{10.95}$$

K_{ID} is a material property dependent on crack speed. Note that K_{ID} is different from K_{Id}, the dynamic fracture toughness for crack initiation in Eq. (10.65). Moreover, $K_{ID}(0) = \lim_{V\to 0} K_{ID}(V)$ is generally not equal to K_{Ic}.

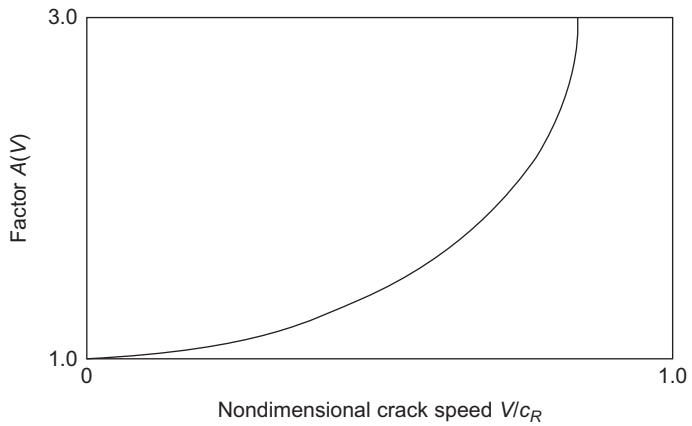

FIGURE 10.9

Variation of factor $A(V)$ with nondimensional crack propagation speed.

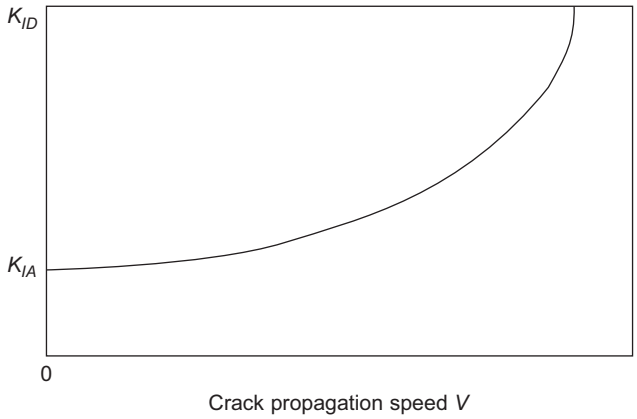

FIGURE 10.10

Schematic of relationship between fracture propagation toughness K_{ID} and crack propagation speed V.

Experimental investigations of Kanazawa and Machida [10-20] and Rosakis and Freund [10-21] for steels showed that K_{ID} is relatively insensitive to V at low crack speeds and increases dramatically with an increase in crack speed when the speed approaches a limiting, material-dependent value. This kind of behavior of K_{ID} as a function of crack speed is schematically shown in Figure 10.10.

Figure 10.10 shows that the fracture propagation toughness K_{ID} approaches K_{IA} in the limit of vanishing crack speed. K_{IA} is generally called fracture arrest toughness and is the minimum value of $K_{ID}(V)$. The crack arrest occurs when the DSIF drops below K_{IA}, that is,

$$K_I(t) < K_{IA} \tag{10.96}$$

10.3.4 Yoffe Crack

As a result of mathematical complexities, closed-form solutions are available for only a few rapid crack propagation problems. Yoffe [10-22] considered a simplified crack model in which a crack of constant length $2a$ propagates at a constant speed V in an infinite plate subjected to a remote tensile loading σ as shown in Figure 10.11. Clearly Yoffe's model is not realistic as the left tip of the crack is required to close during propagation to maintain a constant crack length, which implies that the SIF should be equal to zero at the left tip.

Yoffe obtained the solution of the problem using a Fourier transform method. Here we introduce a complex potential technique for the solution. We begin with Eq. (10.68) for the displacement potentials, which are still valid but now we assume that the rectangular coordinate system (x_1, y_1) is attached to the center of the moving crack with the crack tips at $x_1 = \pm a$, $y_1 = 0$, respectively. Using the superposition method, the boundary conditions for the Yoffe problem in the moving coordinate

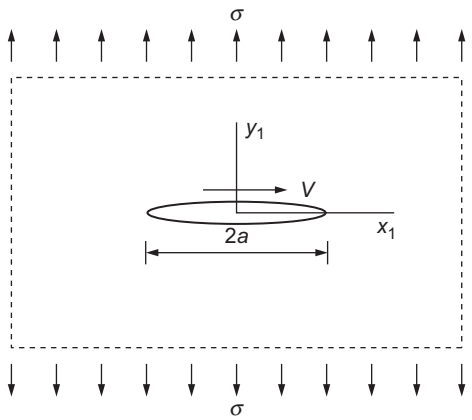

FIGURE 10.11

Yoffe crack: a crack of constant length $2a$ propagating at a constant speed V in an infinite plate.

system can be formulated as follows:

$$\begin{aligned} \sigma_{yy} &= -\sigma, \quad \sigma_{xy} = 0, \qquad 0 \le |x_1| \le a,\ y_1 = 0 \\ u_y &= 0, \qquad \sigma_{xy} = 0, \qquad a < |x_1| < \infty,\ y_1 = 0 \\ \sigma_{xx},\ \sigma_{yy},\ \sigma_{xy} &\to 0, \qquad \sqrt{x_1^2 + y_1^2} \to \infty \end{aligned} \tag{10.97}$$

Under steady state crack propagation conditions, the terms on the right side of Eq. (10.68) vanish and the equations reduce to

$$\begin{aligned} \frac{\partial^2 \varphi}{\partial x_1^2} + \frac{\partial^2 \varphi}{\partial (\alpha_1 y_1)^2} &= 0 \\ \frac{\partial^2 \psi}{\partial x_1^2} + \frac{\partial^2 \psi}{\partial (\alpha_2 y_1)^2} &= 0 \end{aligned} \tag{10.98}$$

These are Laplace equations in the coordinate systems of $(x_1, \alpha_1 y_1)$ and $(x_1, \alpha_2 y_1)$, respectively. Hence, φ can be associated with the real part of a complex function $F_1(z_1)$, and ψ with the imaginary part of a complex function $F_2(z_2)$, that is,

$$\begin{aligned} \varphi &= \varphi(x_1, \alpha_1 y_1) = F_1(z_1) + \overline{F_1(z_1)} \\ \psi &= \psi(x_1, \alpha_2 y_1) = i\left[F_2(z_2) - \overline{F_2(z_2)}\right] \end{aligned} \tag{10.99}$$

where a bar over a quantity denotes its complex conjugate, and

$$\begin{aligned} z_1 &= x_1 + i(\alpha_1 y_1) \\ z_2 &= x_1 + i(\alpha_2 y_1) \end{aligned} \tag{10.100}$$

Using these complex potentials, the displacements and stresses can be expressed in the following forms (Gladwell [10-23]):

$$\begin{aligned} u_x + iu_y = (1-\alpha_1)\Phi(z_1) + (1+\alpha_1)\overline{\Phi(z_1)} \\ + (1-\alpha_2)\Psi(z_2) - (1+\alpha_2)\overline{\Psi(z_2)} \end{aligned} \tag{10.101}$$

$$\begin{aligned} \sigma_{xx} + \sigma_{yy} &= 2\mu\left(\alpha_1^2 - \alpha_2^2\right)\left[\Phi'(z_1) + \overline{\Phi'(z_1)}\right] \\ \sigma_{xx} - \sigma_{yy} + 2i\sigma_{xy} &= 2\mu\Big[(1-\alpha_1)^2\Phi'(z_1) + (1+\alpha_1)^2\overline{\Phi'(z_1)} \\ &\quad + (1-\alpha_2)^2\Psi'(z_2) - (1+\alpha_2)^2\overline{\Psi'(z_2)}\Big] \end{aligned} \tag{10.102}$$

where

$$\Phi(z_1) = F_1'(z_1), \quad \Psi(z_2) = F_2'(z_2)$$

For the Yoffe crack problem, the complex potential functions $\Phi(z_1)$ and $\Psi(z_2)$ can be chosen as (Fan [10-24])

$$\begin{aligned} \Phi'(z_1) &= \frac{\sigma}{2\mu}\frac{1+\alpha_2^2}{4\alpha_1\alpha_2 - \left(1+\alpha_2^2\right)^2}\left(\frac{z_1}{\sqrt{z_1^2 - a^2}} - 1\right) \\ \Psi'(z_2) &= \frac{\sigma}{2\mu}\frac{2\alpha_1}{4\alpha_1\alpha_2 - \left(1+\alpha_2^2\right)^2}\left(\frac{z_2}{\sqrt{z_2^2 - a^2}} - 1\right) \end{aligned} \tag{10.103}$$

Substituting this into the stress expressions Eq. (10.102) along the crack line ($x_1 > a$, $y_1 = 0$, $z_1 = z_2 = x_1$), we have

$$\begin{aligned} \sigma_{xx} + \sigma_{yy} &= 2\mu\left(\alpha_1^2 - \alpha_2^2\right)\frac{2\sigma}{2\mu}\frac{1+\alpha_2^2}{4\alpha_1\alpha_2 - \left(1+\alpha_2^2\right)^2}\left(\frac{x_1}{\sqrt{x_1^2 - a^2}} - 1\right) \\ \sigma_{xx} - \sigma_{yy} + 2i\sigma_{xy} &= 2\mu\left[2 + 2\alpha_1^2\right]\frac{\sigma}{2\mu}\frac{1+\alpha_2^2}{4\alpha_1\alpha_2 - \left(1+\alpha_2^2\right)^2}\left(\frac{x_1}{\sqrt{x_1^2 - a^2}} - 1\right) \\ &\quad 2\mu\left[-4\alpha_2\right]\frac{\sigma}{2\mu}\frac{2\alpha_1}{4\alpha_1\alpha_2 - \left(1+\alpha_2^2\right)^2}\left(\frac{x_1}{\sqrt{x_1^2 - a^2}} - 1\right) \end{aligned} \tag{10.104}$$

The normal stress σ_{yy} along the crack line can be obtained as follows:

$$\sigma_{yy}(x_1,0) = \sigma\left[\frac{x_1}{\sqrt{x_1^2 - a^2}} - 1\right], \quad x_1 > a$$

which is independent of crack propagation speed. Hence, the DSIFs at both crack tips are also independent of crack speed and have the same expression as that for the corresponding quasistatic crack, that is,

$$K_I = \lim_{x_1 \to a^+} \sqrt{2\pi(x_1 - a)}\sigma_{yy}(x_1,0) = \sigma\sqrt{\pi a} \tag{10.105}$$

References

[10-1] S.G. Lekhnitskii (translated by P. Fern), Theory of Elasticity of an Anisotropic Elastic Body, Holden-Day, San Francisco, 1963.

[10-2] G.C. Sih, H. Liebowitz, Mathematical theories of brittle fracture, in: H. Liebowitz (Ed.), Fracture, Vol. 2, Academic Press, New York, 1968, pp. 67–190.

[10-3] G.J. Weng, Some elastic properties of reinforced solids with special reference to isotropic ones containing spherical inclusions, Int. J. Eng. Sci. 22 (1984) 845–856.

[10-4] Z.-H. Jin, N. Noda, Crack-tip singular fields in nonhomogeneous materials, J. Appl. Mech. 61 (1994) 738–740.

[10-5] M.L. Williams, On the stress distribuion at the base of a stationary crack, J. Appl. Mech. 24 (1957) 109–114.

[10-6] J.W. Eischen, Fracture of nonhomogeneous materials, Int. J. Fract. 34 (1987) 3–22.

[10-7] Z.-H. Jin, R.C. Batra, Some basic fracture mechanics concepts in functionally graded materials, J. Mech. Phys. Sol. 44 (1996) 1221–1235.

[10-8] Z.-H. Jin, C.T. Sun, Integral representation of energy release rate in graded materials, J. Appl. Mech. 74 (2007) 1046–1048.

[10-9] T. Honein, G. Herrmann, Conservation laws in nonhomogeneous plane elastostatics, J. Mech. Phys. Sol. 45 (1997) 789–805.

[10-10] F. Delale, F. Erdogan, On the mechanical modeling of an interfacial region in bonded half-planes, J. Appl. Mech. 55 (1988) 317–324.

[10-11] G.C. Sih, Mechanics of Fracture, Vol. 4: Elastodynamic Crack Problems, Noordhoff International Publishing, Leyden, 1977.

[10-12] L.B. Freund, Dynamic Fracture Mechanics, Cambridge University Press, Cambridge, UK, 1990.

[10-13] A.W. Maue, Die entspannungswelle bei plotzlichem Einschnitt eines gespannten elastischen Korpers, Zeitschrift fur angewandte Mathematik und Mechanik, 34 (1954) 1–12.

[10-14] G.C. Sih, G.T. Embley, R.S. Ravera, Impact response of a finite crack in plane extension, Int. J. Sol. Struct. 8 (1972) 977–993.

[10-15] J.R. Rice, Mathematical analysis in the mechanics of fracture, in: H. Liebowitz (Ed.), Fracture, Vol. 2, Academic Press, New York, 1968, pp. 191–311.

[10-16] L.B. Freund, R.J. Clifton, On the uniqueness of plane elastodynamic solutions for running cracks, J. Elast. 4 (1974) 293–299.

[10-17] F. Nilsson, A note on the stress singularity at a non-uniformly moving crack tip, J. Elast. 4 (1974) 73–75.

[10-18] L.B. Freund, Crack propagation in an elastic solid subjected to general loading 2, nonuniform rate of extension, J. Mech. Phys. Sol. 20 (1972) 141–152.

[10-19] F. Nilsson, Dynamic stress intensity factors for finite strip problems, Int. J. Fract. Mech. 8 (1972) 403–411.

[10-20] T. Kanazawa, S. Machida, Fracture dynamics analysis on fast fracture and crack arrest experiments, in: T. Kanazawa, A.S. Kobayashi, K. Ido (Eds.), Fracture Tolerance Evaluation, Toyoprint, Japan, 1982.

[10-21] A.J. Rosakis, L.B. Freund, Optical measurement of the plastic strain concentration at a crack tip in a ductile steel plate, J. Eng. Mater. Technol. 104 (1982) 115–120.

[10-22] E.H. Yoffe, The moving Griffith crack, Philos. Mag. 42 (1951) 739–750.

[10-23] G.M.L. Gladwell, On the solution of problems of dynamic plane elasticity, Mathematika 4 (1957) 166–168.

[10-24] T.Y. Fan, Moving Dugdale model, Zeitschrift fur angewante Mathematik und Physik 38 (1987) 630–641.

[10-25] C. Atkinson, J.D. Eshelby, The flow of energy into the tip of a moving crack, Int. J. Fract. Mech. 4 (1968) 3–8.